Simultaneous batholith emplacement, terrane/continent collision, and oroclinal bending in the Blue Mountains Province, North American Cordillera: Oroclinal Bending in the Blue Moun…

ARTICLE *in* TECTONICS · JUNE 2015

Impact Factor: 3.32 · DOI: 10.1002/2015TC003859

6 AUTHORS, INCLUDING:

Filip Tomek

Charles University in Prague

10 PUBLICATIONS **14** CITATIONS

SEE PROFILE

František Holub

Charles University in Prague

27 PUBLICATIONS **484** CITATIONS

SEE PROFILE

Kenneth Johnson

University of Houston - Downtown

16 PUBLICATIONS **185** CITATIONS

SEE PROFILE

Joshua Schwartz

California State University, Northridge

36 PUBLICATIONS **635** CITATIONS

SEE PROFILE

AGU PUBLICATIONS

Tectonics

RESEARCH ARTICLE
10.1002/2015TC003859

Key Points:
- Wallowa batholith was emplaced during protracted terrane/continent collision
- Blue Mountains superterrane impinged into a continental reentrant
- Pluton fabrics record Early Cretaceous onset of oroclinal bending

Supporting Information:
- Tables S1–S4
- Parts S1–S7

Correspondence to:
J. Žák,
jirizak@natur.cuni.cz

Citation:
Žák, J., K. Verner, F. Tomek, F. V. Holub, K. Johnson, and J. J. Schwartz (2015), Simultaneous batholith emplacement, terrane/continent collision, and oroclinal bending in the Blue Mountains Province, North American Cordillera, *Tectonics*, *34*, doi:10.1002/2015TC003859.

Received 16 FEB 2015
Accepted 4 MAY 2015
Accepted article online 8 MAY 2015

Simultaneous batholith emplacement, terrane/continent collision, and oroclinal bending in the Blue Mountains Province, North American Cordillera

Jiří Žák[1], Kryštof Verner[2,3], Filip Tomek[1,4], František V. Holub[3], Kenneth Johnson[5], and Joshua J. Schwartz[6]

[1]Institute of Geology and Paleontology, Faculty of Science, Charles University, Prague, Czech Republic, [2]Czech Geological Survey, Prague, Czech Republic, [3]Institute of Petrology and Structural Geology, Faculty of Science, Charles University, Prague, Czech Republic, [4]Institute of Geology, Czech Academy of Sciences, Prague, Czech Republic, [5]Department of Natural Sciences, University of Houston-Downtown, Houston, Texas, USA, [6]Department of Geological Sciences, California State University, Northridge, California, USA

Abstract The North American Cordillera is a classic example of accretionary orogen, consisting of multiple oceanic terranes attached to the western margin of Laurentia during the Mesozoic times. Although the Cordillera is linear for most parts, terrane boundaries are at a high angle to the overall structural grain in several segments of the orogen, which has been a matter of longstanding controversy as to how and when these orogenic curvatures formed. This paper discusses mechanisms, kinematics, and timing of initiation of one of these major curvatures, the Blue Mountains Province in northeastern Oregon. Here magmatic fabric patterns and anisotropy of magnetic susceptibility in the Wallowa batholith record three phases of progressive deformation of the host Wallowa terrane during Early Cretaceous. First is terrane-oblique ~NE-SW shortening, interpreted as recording attachment of the amalgamated oceanic and fringing terranes to the continental margin during dextral convergence at ~140 Ma. Deformation subsequently switched to pure shear-dominated ~NNE-SSW shortening associated with crustal thickening, caused by continued impingement of the amalgamated Blue Mountains superterrane into a presumed westward concave reentrant in the continental margin at ~135–128 Ma. Upon impingement (at ~126 Ma), the northern portion of the superterrane became "locked," leading to reorientation of the principal shortening direction to ~NNW-SSE while its still deformable southern portion rotated clockwise about a vertical axis. We thus propose oblique bending as the main mechanism of the orocline formation whereby horizontal compressive forces resulting from plate convergence acted at an angle to the terrane boundaries.

1. Introduction

The North American Cordillera developed as an accretionary orogen along the western margin of Laurentia during the Mesozoic to Cenozoic times (Figure 1) [e.g., *Coney et al*., 1980; *Monger*, 1997; *Dickinson*, 2004; *Piercey and Colpron*, 2009; *Hildebrand*, 2013]. Although the polarity and significance of the past subductions have been a matter of debate [e.g., *Johnston*, 2008; *Hildebrand*, 2009, 2013; *Sigloch and Mihalynuk*, 2013], the prevailing view is that the overall eastward motion of the paleo-Pacific basin [e.g., *Hamilton*, 1969; *Atwater*, 1970; *Engebretson et al*., 1985], itself composed of several oceanic plates, brought a number of Late Paleozoic to Early Mesozoic intraoceanic-arc systems and associated sedimentary basins (in some reconstructions inferred to compose a large ribbon continent) [e.g., *Johnston*, 2001, 2008; *Hildebrand*, 2009, 2013] to the proximity of the Laurentian margin. These oceanic units were then successively attached to and variously displaced along this continental margin as tectonostratigraphic terranes (Figure 1). Much of the western North American Cordillera is linear and roughly parallels the leading continental edge, however, some portions exhibit a significant curvature and are at a high angle to the overall ~NNW-SSE tectonic grain (Figure 1; present-day coordinates are used throughout this paper). From north to south, the major Cordilleran orogenic curvatures include the Bering Strait region northwest of Alaska [e.g., *Patton and Tailleur*, 1977; *Amato et al*., 2004] (not shown in Figure 1), several oroclines in central and southern Alaska [e.g., *Johnston*, 2001; *Glen*, 2004], the Southern Vancouver Island orocline [*Johnston and Acton*, 2003], the Blue Mountains Province (Figure 1), forming what was variously referred to as the Columbia or Idaho orocline [e.g., *Carey*, 1958; *Hamilton and Myers*, 1966; *Taubeneck*, 1966;

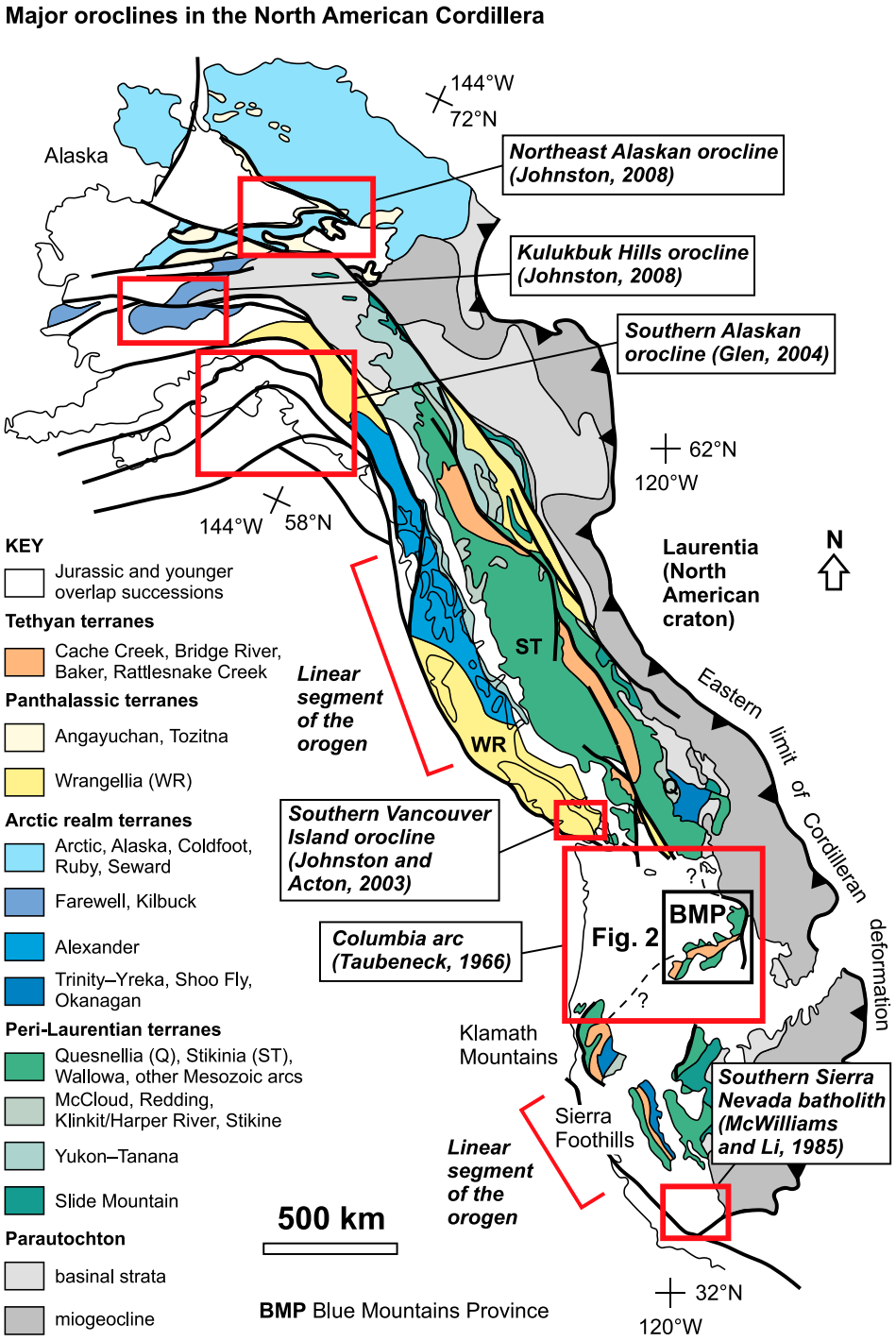

Figure 1. Schematic geologic map showing the principal tectonostratigraphic terranes, their inferred afinities, and major oroclines in the North American Cordillera. Base map modified from *Piercey and Colpron* [2009].

Greenwood and Reid, 1969] around an area covered by Tertiary volcanic and sedimentary rocks (Figure 1), and an orocline at the southern termination of the Sierra Nevada batholith [*McWilliams and Li*, 1985].

As exemplified by the Blue Mountains Province, large uncertainty persists regarding the driving forces, kinematics, exact amount of rotation, and timing of formation of these orogenic curvatures. In this paper, we examine in detail a portion of the Early Cretaceous Wallowa batholith that, on a regional scale, intrudes the "hinge" of the Blue Mountains orocline (Figures 2 and 3). Furthermore, the existing structural and

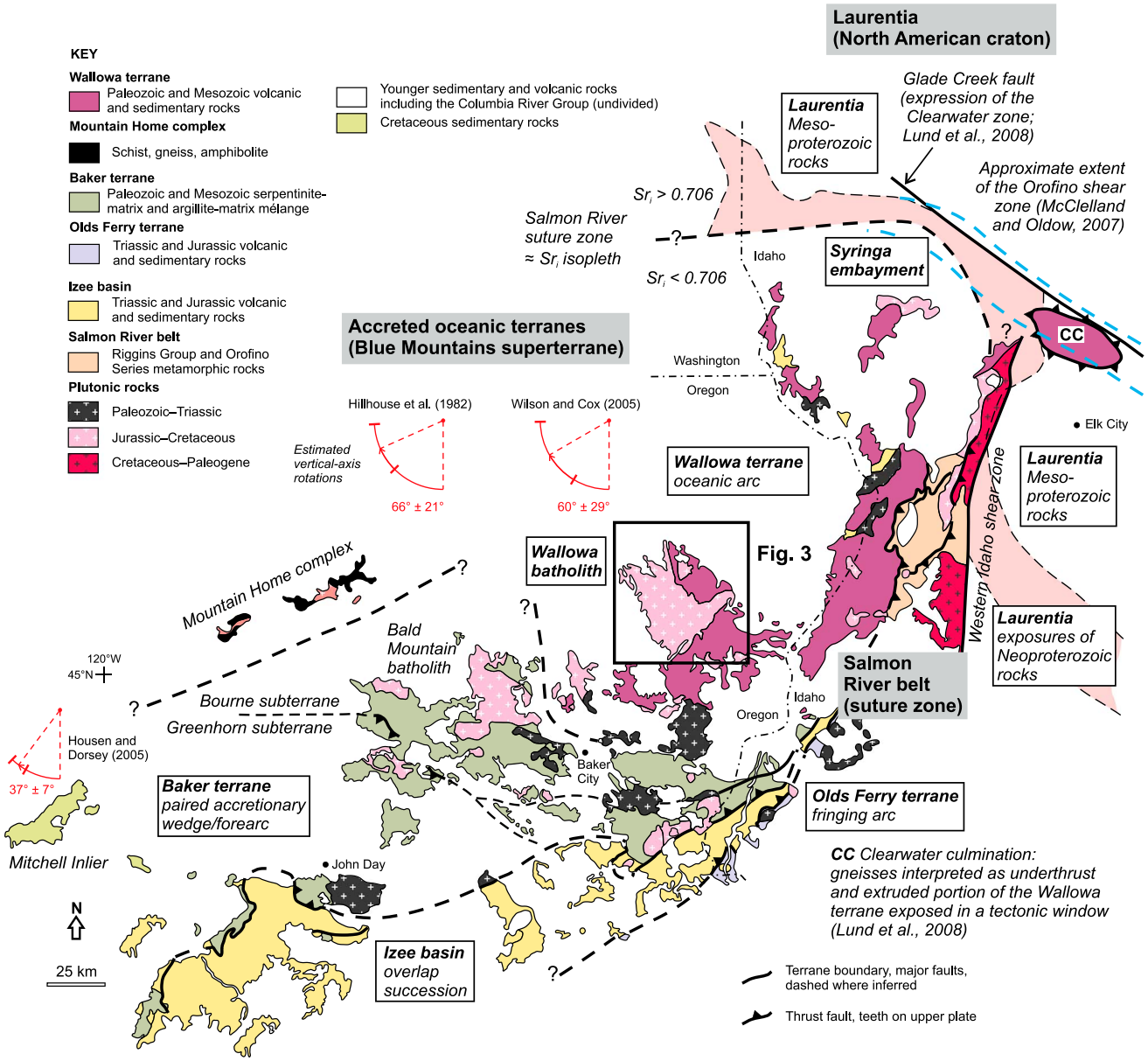

Figure 2. Simplified geologic map showing terranes, their boundaries, other principal tectonic features, and main plutonic units in the Blue Mountains Province accreted to the North American craton. The Wallowa batholith intruded into the hinge of the orogenic curvature. Redrafted from *Schwartz et al.* [2011a].

geochronologic data establish that batholith emplacement was broadly coeval with collision of the previously amalgamated oceanic terranes ("the Blue Mountains superterrane"; Figure 2) with the North American craton. The Wallowa batholith is thus one of the key areas to explore the nature of crustal deformation, kinematics, and temporal relations of plutonism to terrane/continent collision and to vertical-axis lithospheric rotations in the Cordilleran orogen.

Below, we first briefly review the principal tectonic elements of the Blue Mountains Province and geology of the Wallowa batholith and then concentrate on the host rock deformation structures and multiple magmatic to solid-state fabrics recorded in the batholith. The field observations are complemented by a magnetic fabric analysis in three main component plutons of the batholith to obtain an independent quantitative information on their internal structure and to infer possible strain patterns recorded by these plutons. Finally, we use these data sets as a background for discussion on kinematics and potential geodynamic causes of the vertical-axis lithospheric rotations in the North American Cordillera.

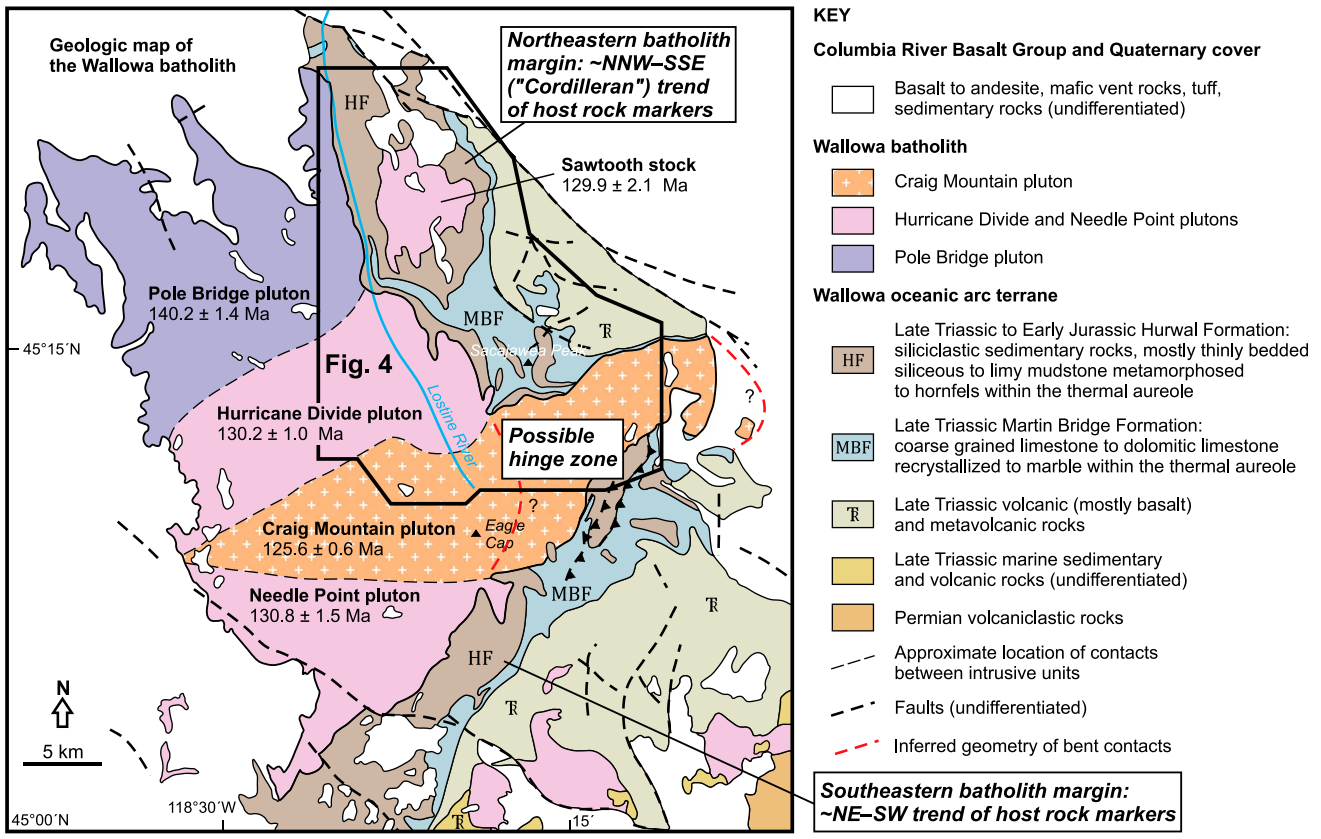

Figure 3. Simplified geologic map of the Wallowa batholith, which is largely concealed beneath the Tertiary Columbia River Basalt Group. The batholith is composite and consists of four component intrusions emplaced over a time span of about 15 Myr during Early Cretaceous. Geology compiled from *Walker* [1979] and *Taubeneck* [1987] and radiometric ages from *Johnson et al.* [2011].

2. Principal Lithotectonic Elements of the Blue Mountains Province

2.1. Overview

The Blue Mountains Province is an erosional inlier that exposes the uplifted Late Paleozoic to Mesozoic variably metamorphosed basement rocks from beneath Tertiary and Quaternary deposits and Columbia River flood basalts. The basement comprises the following principal lithotectonic units [e.g., *Dorsey and LaMaskin*, 2007, 2008; *LaMaskin et al.*, 2009, 2011; *Schwartz et al.*, 2010, 2011a]:

1. The outboard Wallowa terrane (Figure 2) is an oceanic island arc assemblage consisting of Permian and Triassic volcanic and volcaniclastic rocks. The island arc volcanic complex is overlain unconformably by Triassic to Lower Jurassic siliciclastic and limestone successions of the Hurwal and Martin Bridge Formations, respectively [e.g., *Stanley et al.*, 2008], and these rocks are in turn unconformably overlain by a Middle to Upper Jurassic flysch-like succession [*LaMaskin et al.*, 2008]. The Wallowa terrane was correlated with the Wrangellia or Stikinia terranes farther north in the Canadian Cordillera [e.g., *Sarewitz*, 1983; *Mortimer*, 1986; *Wernicke and Klepacki*, 1988; *Schwartz et al.*, 2011a].
2. The less extensively exposed, inboard Olds Ferry terrane (Figure 2) is also an island arc complex that consists of Middle Triassic to Lower Jurassic weakly metamorphosed volcanic and volcaniclastic rocks of chiefly andesitic composition [*Brooks and Vallier*, 1978; *Vallier*, 1995]. This terrane was interpreted as a fringing arc complex that developed along the North American passive margin [e.g., *Ferns and Brooks*, 1995].
3. The Baker terrane (Figure 2) is a subduction–accretionary wedge–fore-arc complex located between the two island arc assemblages and was thrust over the Wallowa terrane during Middle to Late Jurassic terrane convergence [*Ferns and Brooks*, 1995; *Schwartz et al.*, 2010; *Žák et al.*, 2012a]. The terrane contains fault-bounded island arc igneous and sedimentary rocks ranging in age from Middle Devonian to Early Jurassic and extensively disrupted fragments of ocean floor, including mélanges with blocks of

moderate-pressure metamorphic rocks [*Schwartz et al*., 2011a]. Part of the Baker terrane is overlain unconformably by a Permian to Triassic siliciclastic successions [*Ferns and Brooks*, 1995; *Schwartz et al*., 2011a].

4. The Izee unit (Figure 2) comprises Triassic and Jurassic sedimentary successions that can be divided into two marine siliciclastic Upper Triassic to Early to early Late Lower Jurassic megasequences separated by an angular unconformity [*Dorsey and LaMaskin*, 2007]. The Izee basin was earlier interpreted as a separate fore-arc basin terrane [*Dickinson*, 1979] but recently was reinterpreted as a regional overlap succession that rests unconformably upon the Baker and Olds Ferry terranes [*Dorsey and LaMaskin*, 2007].
5. To the east, the Blue Mountains oceanic terranes are juxtaposed against the western margin of the North American craton (Laurentia) along the Salmon River suture zone (Figure 2). This zone comprises several west dipping thrust sheets derived from the Wallowa terrane, pinches out the Baker and Olds Ferry terranes, and is separated from the easterly Cretaceous-Tertiary plutons of the Idaho batholith along the Western Idaho shear zone. The Salmon River suture zone also coincides with the $^{0.706}$Sr line which marks an abrupt increase in contamination of plutonic rocks by radiogenic Precambrian continental crust [e.g., *Armstrong et al*., 1977; *Manduca et al*., 1992, 1993; *Giorgis et al*., 2005].

Although the Salmon River suture zone records a protracted kinematic history [e.g., *Manduca et al*., 1993; *McClelland et al*., 2000; *Gray and Oldow*, 2005; *Giorgis et al*., 2008], most relevant for this study are the Early Cretaceous events coeval with emplacement of the Wallowa batholith. Recent petrologic data and Sm-Nd garnet ages suggest prograde amphibolite-facies metamorphism and garnet growth at ~141–124 Ma and were interpreted as recording crustal thickening via stacking of thrust sheets and dating the collision of the previously amalgamated terranes with the western North American margin [*Selverstone et al*., 1992; *Getty et al*., 1993; *McKay*, 2011; *Stowell et al*., 2014].

(6) To the northeast, the Wallowa terrane, Salmon River belt, and Western Idaho shear zone abut against the North American craton margin. In the map (Figure 2), all these units as well as the Sr_i isopleth take an abrupt, approximately 90° bend from ~NNE-SSW in the east to ~E-W in the north; the bend has been referred to as the Syringa embayment. The origin of the bend has been a matter of controversy (see *Lund et al*. [2008] for discussion). In one view, the embayment is an inherited preaccretion feature of the rifted North American craton margin [*Schmidt et al*., 2003, 2009] with the ~E-W segment representing a transform fault and the ~NNE-SSW segment representing part of the now shortened rift structure [*Tikoff et al*., 2014]. Recent paleomagnetic data suggest that the original orientation of the two segments may have been 60° and 330°, respectively [*Tikoff et al*., 2014]. In an opposite view, formation of the bend is a result of sinistral transpressional shearing where the NNE-SSW trending assemblages have been truncated along the Late Cretaceous ~NW-SE to ~E-W trending Orofino shear zone (Figure 2; active from ~90 to ~70 Ma) [*McClelland and Oldow*, 2007].

2.2. Geometry of the Terrane Boundaries and Vertical-Axis Block Rotations

In a regional map view, the terrane boundaries in the Blue Mountains Province generally trend ~E-W in the west and then continuously reorient to the ~NNE-SSW trend in the east (Figure 2). The ~E-W trend of the Blue Mountains terranes is at a high angle to the ~NNW-SSE trend of the Sierra Nevada and Canadian Cordillera terranes (Figure 1). The curved terrane boundaries in the Blue Mountains Province are thus suggestive of significant clockwise vertical-axis rotation (Figure 2), a notion that is supported by several paleomagnetic studies (see *Housen and Dorsey* [2005] for discussion). *Wilson and Cox* [1980] inferred rotation by 60° ± 29° on the basis of samples from plutonic and contact metamorphic rocks of the Wallowa batholith and Baker terrane. Similarly, *Hillhouse et al*. [1982] estimated rotation by 66° ± 21° from Upper Triassic volcanogenic rocks of the Wallowa terrane. Cretaceous sedimentary rocks of the Mitchell Inlier (Figure 2), recently interpreted by *Schwartz and Johnson* [2014] as separated from the central Blue Mountains by a large-magnitude shear zone, indicate a lesser amount of rotation of 37° ± 7°. The rotation was resolved into 21° from the mid-Cretaceous to early/middle Eocene and an additional 16° after Eocene [*Housen and Dorsey*, 2005; see also *Grommé et al*., 1986]. It follows from the above that the paleomagnetic data from igneous and metamorphic rocks lack paleohorizontal control and involve an unknown amount of tilt of the sampled units and that large rotations are consistently derived from older rocks in the Blue Mountains Province; thus, all of the above estimates may be correct.

3. Geology of the Wallowa Batholith

The Wallowa batholith is the largest (~620 km^2) of multiple compositionally diverse plutonic bodies that intruded the Blue Mountains Province (Figure 2) [*Krauskopf*, 1943]. The batholith is composite and from north to south consists of four main plutons (Figures 3 and 4) [*Taubeneck*, 1987; *Johnson et al*., 2011]: Pole Bridge (140.2 ± 1.4 Ma), Hurricane Divide (130.2 ± 1.0 Ma), Craig Mountain (125.6 ± 0.6 Ma), and Needle Point (130.8 ± 1.5 Ma; not examined in this study). Overlapping ages and identical compositions of the ~130 Ma Hurricane Divide and Needle Point plutons (K. Johnson, unpublished data) suggest that they are virtually the same intrusion bifurcated by the younger Craig Mountain pluton (Figure 3). From north to south, the interpluton contacts change orientation from ~NE-SW to ~E-W and define a fan-like pattern, with the youngest Craig Mountain pluton in the middle tapered westward. In addition, the Sawtooth stock dated at 129.9 ± 2.1 Ma (all ages are based on U-Pb sensitive high-resolution ion microprobe–reverse geometry (SHRIMP-RG) measurements of igneous zircons) [*Johnson et al*., 2011] intruded the easterly batholith host rock and is correlative both in terms of composition and age with the Hurricane Divide pluton (Figures 3 and 4).

Rocks from the Pole Bridge, Hurricane Divide, and Sawtooth plutons are broadly of the same lithology, ranging from low-silica tonalite along pluton margins to amphibole-biotite granodiorite in pluton cores. Minor hornblende gabbro bodies intrude all of the tonalite-granodiorite plutons. These plutons are interpreted to be derived from a depleted mantle source during Late Jurassic-Early Cretaceous crustal thickening broadly coeval with thrust loading in the Salmon River belt [*Johnson et al*., 2011]. On the other hand, the Craig Mountain pluton is more felsic and primarily granodiorite. Rocks of the Craig Mountain pluton are consistent with partial melting of thickened crust [*Johnson et al*., 2011] following attachment of the Blue Mountains superterrane to the continental margin at ~141–124 Ma. The last stage of Wallowa magmatism is represented by small satellite bodies of cordierite-bearing trondhjemite to the south of the main batholith [e.g., *Taubeneck*, 1964; *Johnson et al*., 1997, 2002].

In summary, existing geochemical data indicate that the Wallowa batholith formed in a suprasubduction setting associated with amalgamation of the Blue Mountains superterrane to the North American craton [*Johnson et al*., 2011]. However, it remains unclear, and beyond the scope of this paper, whether Wallowa plutonism formed above an oceanic plate subducting eastward (Farallon plate) or westward (oceanic basin once underlying the Salmon River belt) beneath the Blue Mountains superterrane. Contrasting views regarding subduction zone polarity are presented in *Selverstone et al*. [1992], *McClelland et al*. [2000], *Dorsey and LaMaskin* [2007, 2008], and *Schwartz et al*. [2011b, 2014, and references therein].

The remainder of the Wallowa batholith is largely concealed by basalt flows of the Miocene Columbia River Group; intrusive contacts against the host rocks of the Wallowa oceanic arc terrane are exposed only along its northeastern and southeastern margins (Figures 3 and 4) [*Krauskopf*, 1943; *Weis et al*., 1976]. In a stratigraphic order, these variably metamorphosed volcanic and sedimentary arc-related host rocks comprise (1) a Triassic succession, the base of which is not exposed, of altered basic to intermediate volcanic rocks and marine mudstones, sandstones, and conglomerates, overlain conformably by (2) an ~300–460 m thick succession of Upper Triassic (Carnian-Norian) limestone and calcareous shales of the Martin Bridge Formation, and by (3) Upper Triassic to Lower Jurassic (Norian-Sinemurian) bedded siliciclastic sedimentary rocks of the Hurwal Formation comprising shales, siltstones, and quartzites of unknown total thickness [*Weis et al*., 1976; *Stanley et al*., 2008]. Both successions have been heterogeneously overprinted by contact metamorphism which produced a variety of hornfels from siliciclastic protoliths and was most intense in the carbonate lithologies. The latter are commonly recrystallized to marbles and calc-silicate rocks with tremolite, garnet, epidote, diopside, and wollastonite [*Krauskopf*, 1943]. Away from the batholith, the degree of regional metamorphism is low in general and does not exceed greenschist-facies conditions, consistent with Al in hornblende barometry indicating a shallow emplacement depth of less than 7 km [*Žák et al*., 2012b].

4. Structure of the Batholith Host Rock

On a regional map scale, lithologic contacts between the Late Triassic (meta) volcanic rocks and the Martin Bridge and Hurwal Formations define an arc with an ~NNW-SSE trending limb roughly parallel to the northeastern batholith margin, hinge zone located within the northeastern off-shoot of the Craig

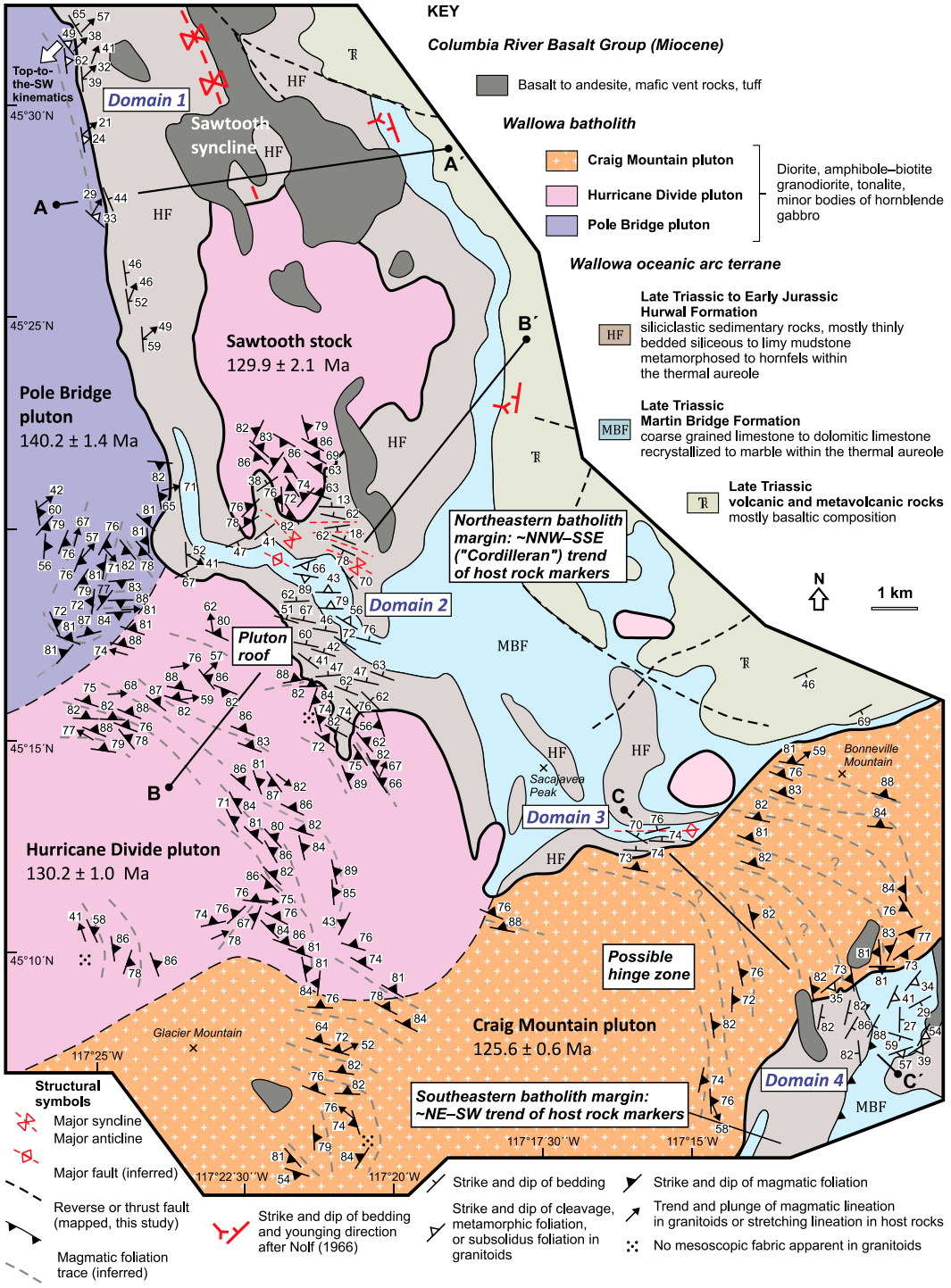

Figure 4. Structural map of the northeastern portion of the Wallowa batholith and its host rocks. Note different magmatic to solid-state fabric patterns in each pluton.

Mountain pluton, and an ~NNE-SSW trending limb parallel to the southeastern batholith margin (Figures 3 and 4). At this scale, the outer batholith margin is largely discordant to bedding and foliation in the host rock, and the interpluton contacts are at a high angle to the regional curvature of host rock markers (Figures 3 and 4).

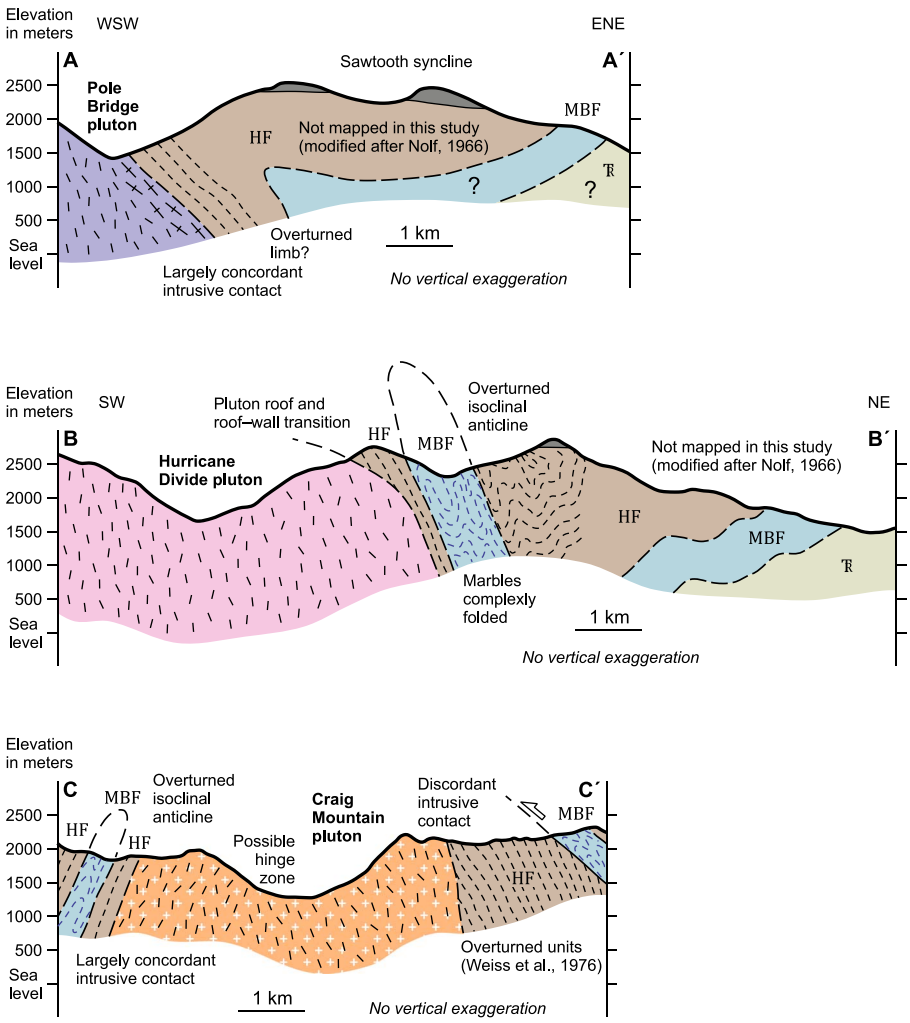

Figure 5. Schematic structural cross sections across the Pole Bridge, Hurricane Divide, and Craig Mountain plutons and their host rocks. See Figure 4 for location.

This tens of kilometers scale structure contains folds on a scale of kilometers to hundreds meters with the fold geometry and fabric orientation varying along strike; in some places, fold limbs have been overturned (Figures 4–7a and 7b). Below, the fabrics and folds are described in four domains from the northwest to the southeast along the batholith margin (Domains 1–4; Figure 4).

In Domain 1, bedding is well preserved, chiefly planar, and oriented uniformly over large regions in the siliciclastic rocks of the Hurwal Formation (Figures 4–6c). Near the Pole Bridge pluton, the bedding strikes parallel to the pluton margin and dips at moderate angle to the ~ENE to ~E, slickenside-type striations on the bedding planes plunge at moderate angle to the ~NNE to ~NE (Figures 4 and 5). This easterly dipping strata are part of a major ~NNW-SSE trending Sawtooth syncline [*Nolf*, 1966; not mapped in this study] (Figures 4 and 5).

In Domain 2, significant vertical relief establishes that the northeastern margin of the Hurricane Divide pluton is a flat-lying batholith roof (Figure 6a) rolling over into a steep wall (see *Žák et al*. [2012b] for details). The overall synclinal architecture described above is here superposed by smaller-scale folds with their axial planes at a high angle to the ~NNW-SSE structural grain (Figures 4 and 6b). For instance, we mapped a steeply inclined, tight to isoclinal, ~NNW-SSE to ~NW-SE trending anticline facing toward the pluton, where the marbles and calc-silicate rocks of the Martin Bridge Formation occupy the core and the overlying siliciclastic rocks of the Hurwal Formation are exposed in the limbs (Figures 4–6b). Furthermore,

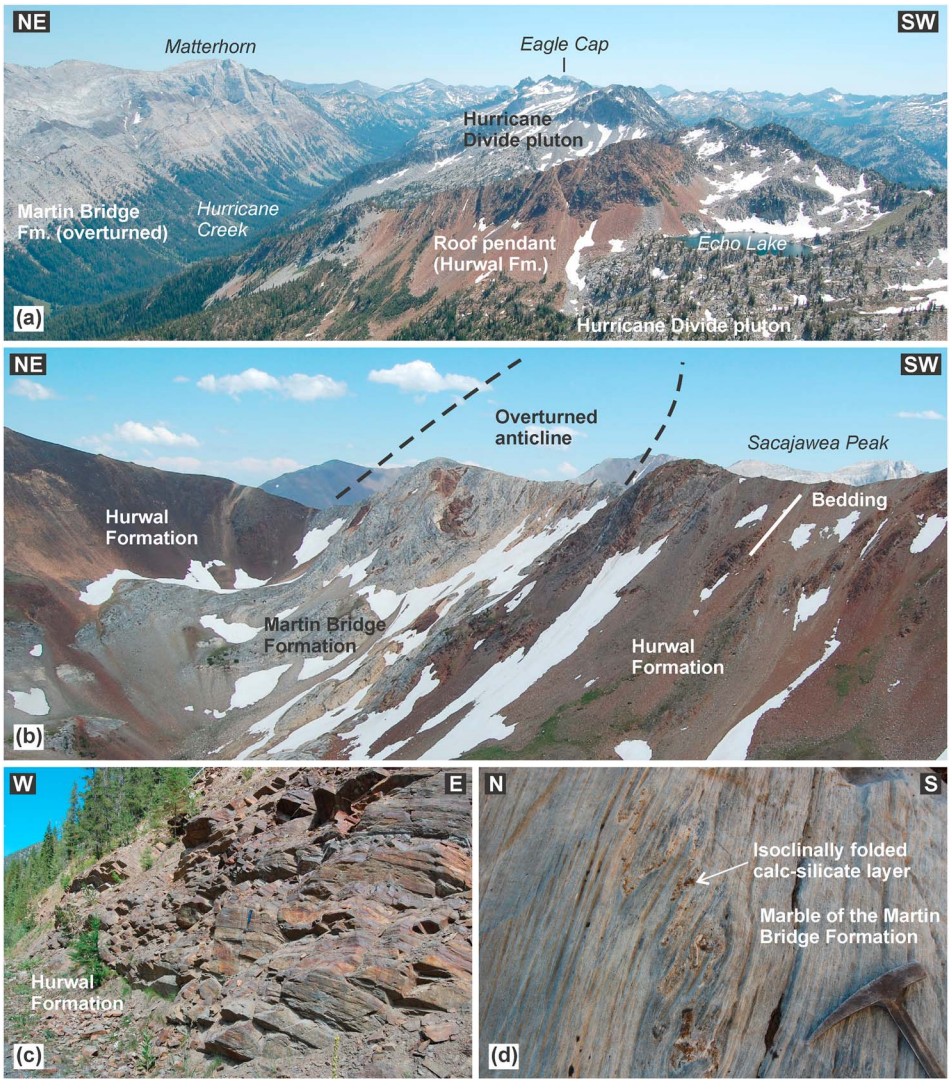

Figure 6. Host rock structures along the northeastern margin of the Wallowa batholith. (a) Distant view to the SE on top of the Wallowa batholith with a flat roof pendant made up of the siliciclastic rocks of the Hurwal Formation and east dipping marbles of the Martin Bridge Formation in the far left background; view from a ridge in the Hurricane Divide. (b) Overturned NW-SE trending isoclinal anticline cored by marbles of the Martin Bridge Formation, looking SE; ridge 2.2 km SSE of Frances Lake. (c) East dipping bedded siliciclastic succession of the Hurwal Formation; hammer for scale. World Geodetic System (WGS84) coordinates: N45.340177°, W117.410447°. (d) Minor isoclinal folds with their axial planes parallel to pervasive metamorphic foliation in marble of the Martin Bridge Formation; hammer for scale. WGS coordinates: N45.27841455°, W117.35172400°.

another anticlines and synclines occur in the nearby Hurwal Formation (Figures 4 and 5). The exception to this generally simple fold style is seen in the marbles where boudins of calc-silicate rocks have been folded more complexly. On outcrops, both formations exhibit remarkably contrasting patterns of deformation (Figures 6c and 6d). The marbles exhibit pervasive metamorphic foliation and compositional banding (Figure 6d) and have well-developed mineral and stretching lineations defined by elongated or fibrous grains and aggregates of calcite, tremolite, and epidote. Foliation commonly encloses boudins of competent calc-silicate rocks and is axial planar to minor tight to isoclinal folds defined by folded calcite veins or quartzite and calc-silicate intercalations (Figure 6d). Farther south, bedding in the siliciclastics and metamorphic foliation and banding in the marbles strike ~E-W to ~NW-SE and dip moderately to steeply to the ~N to ~NE (Figures 4, 5, and 7a). Mineral lineation in the marbles tends to plunge moderately to the ~NE (Figures 4 and 7a).

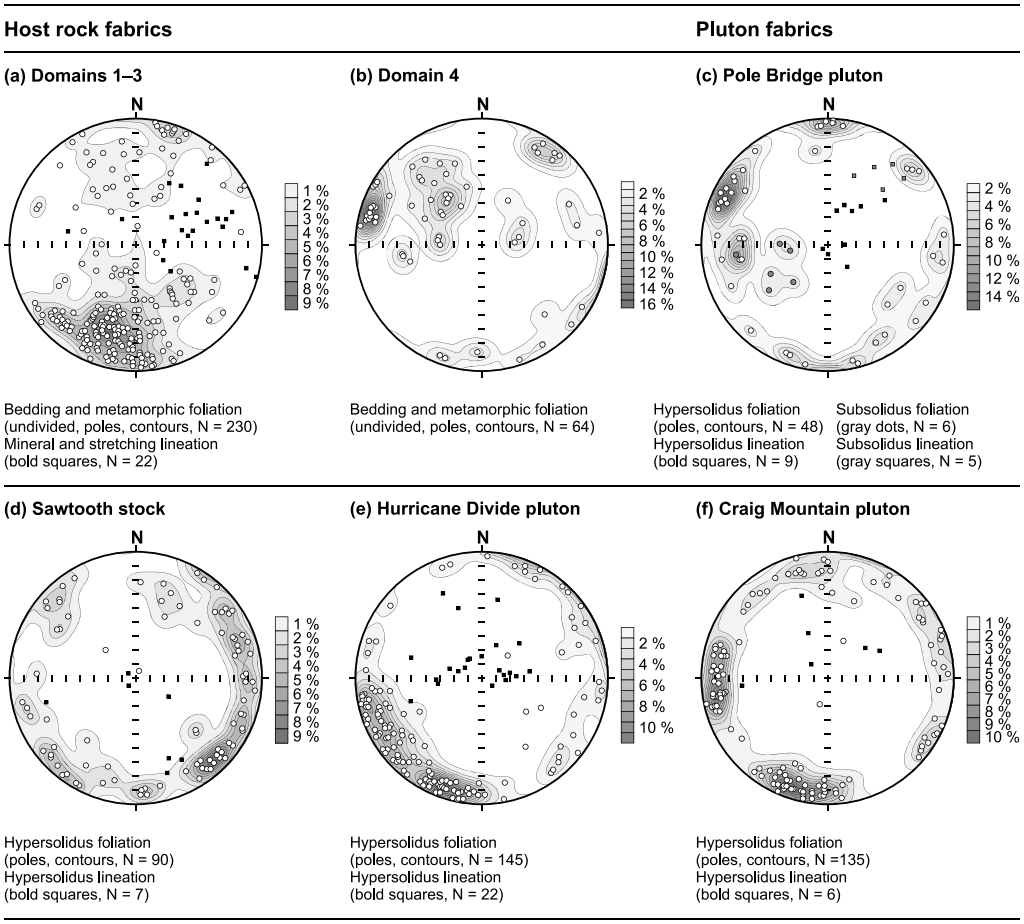

Figure 7. Stereonets (equal area projection, lower hemisphere) showing orientation of fabric elements in the Wallowa terrane and in component plutons of the Wallowa batholith.

In Domain 3 along the northwestern margin of the Craig Mountain pluton, lithologic contacts between the Martin Bridge and Hurwal Formations, as well as steep metamorphic foliation and bedding, dip steeply to the north and, again, appear deflected from the ~NNW-SSE to the ~E-W strike, i.e., toward parallelism with the nearby pluton margin (Figures 4 and 5). Similarly to Domain 2, the units here define an overturned steep isoclinal anticline cored by the marbles and facing toward the pluton (Figures 4 and 5).

In the southeasterly Domain 4, a limb-parallel, ~NNE-SSW trending reverse to thrust fault was mapped that separates siliciclastic rocks of the Hurwal Formation from the Martin Bridge marbles (Figures 4 and 5). Bedding and foliation dip moderately to steeply to the ~ESE to ~SE (Figures 4, 5, and 7b), and mineral and stretching lineations are rare. In contrast to Domain 3, the intrusive pluton/host rock contact is discordant and truncates both the thrust fault and mesoscopic fabrics in the host rock.

5. Multiple Magmatic to Solid State Fabrics in the Wallowa Batholith

Mesoscopic magmatic foliation in the Pole Bridge, Hurricane Divide, and Craig Mountain plutons is commonly defined by planar shape-preferred orientation of biotite, hornblende, and feldspar grains or aggregates (Figure 8a) and by the alignment of flattened microgranular enclaves and elongated host rock xenoliths (Figures 8a–8d). Lineation is defined by linear shape-preferred orientation of euhedral to subhedral hornblende crystals or elongated biotite aggregates in the foliation plane. On many outcrops, however, lineation is difficult to measure due to the lack of suitably oriented, foliation-parallel surfaces.

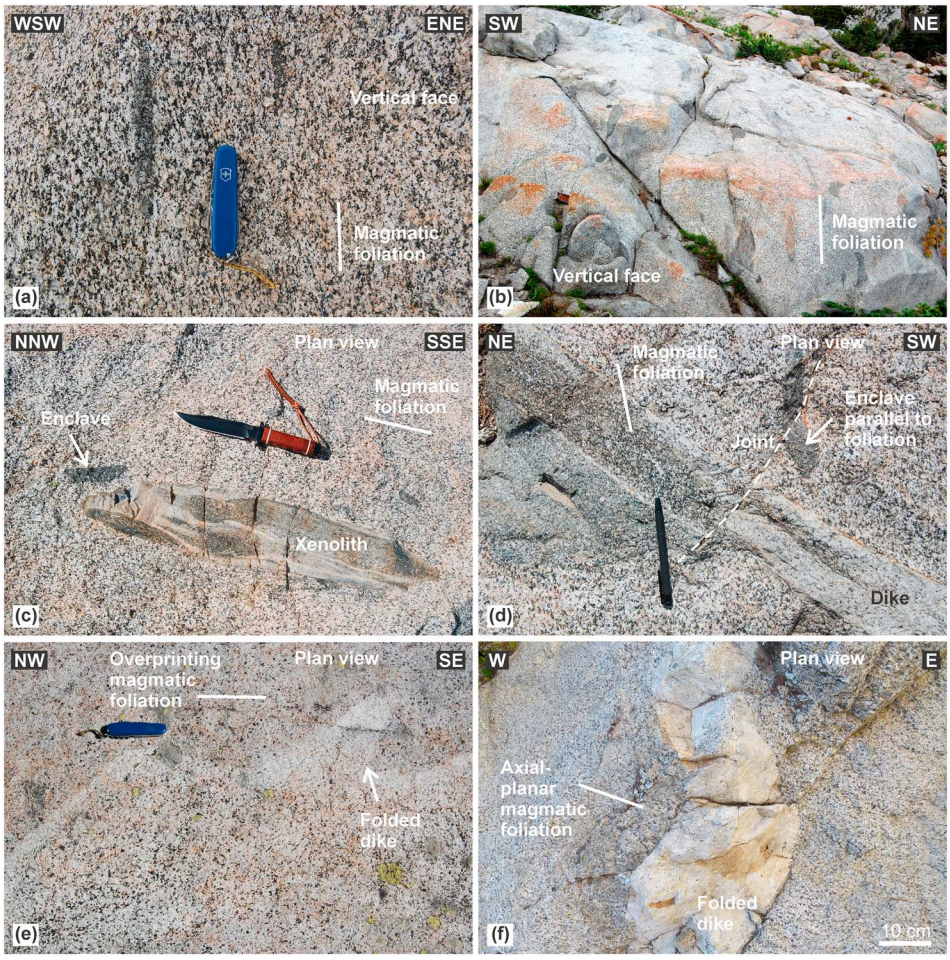

Figure 8. Field examples of magmatic fabrics in the Wallowa batholith and their geometric and temporal relations to other magmatic structures. (a) Close-up of subvertical mineral foliation in the Hurricane Divide pluton, defined mainly by amphibole and biotite. Stretched microgranular enclave is aligned parallel to the mineral fabric in the host granodiorite. Swiss Army penknife for scale is 9 cm long. WGS84 coordinates: N45.24463205°, W117.34662060°. (b) Steeply dipping swarm of flattened microgranular enclaves aligned parallel to mineral foliation in the host granodiorite of the Hurricane Divide pluton. WGS84 coordinates: N45.25134667°, W117.4067383°. (c) Microgranular enclave near larger host rock xenolith, both with their long axes parallel to mineral foliation in the host granodiorite of the Hurricane Divide pluton. SOG 2.0 Bowie knife for scale is 28 cm long. WGS84 coordinates: N45.24509900°, W117.34090380°. (d) Close-up of mineral fabric overprinting at a high angle a composite aplitic-mafic cumulate dike. Note microgranular enclave parallel to the host mineral fabric; the Hurricane Divide pluton. Pencil for scale is 14 cm long. WGS84 coordinates: N45.24362002°, W117.34236385°. (e) Mineral fabric in the host granodiorite overprinting a folded aplitic dike. Swiss Army penknife for scale is 9 cm long. WGS84 coordinates: N45.21056347°, W117.3931542°. (f) Aplitic dike folded into an open magmatic fold, magmatic foliation in the host granodiorite is axial planar to this fold; the Craig Mountain pluton. WGS coordinates: N45.201704°, W117.208478°.

A similar feature of all plutons in the batholith is a moderately to steeply plunging lineation (~60–90° plunge) and a steep foliation (~70–90° dip), the strike and statistical orientation distribution of which varies among the individual plutons (Figures 4 and 7c–7f). In most cases, poles to foliation tend to concentrate around the periphery of the stereonets with multiple maxima and submaxima (Figures 7c–7f) and thus define a girdle around the steeply plunging lineation. The Pole Bridge pluton is characterized by margin-parallel, ~N to ~NNW striking subsolidus foliation in the north and two distinct foliations (~NNE-SSW and ~E-W) in its southeastern portion (Figures 4 and 7c). Broadly similar to the latter is the Sawtooth stock with dominant ~NE-SW and less pronounced ~NW-SE foliations (Figures 4 and 7d). In the Hurricane Divide pluton, foliation strikes predominantly ~WNW-ESE and ~NW-SE but also ~N-S to ~NNE-SSW in a domain near its southern margin (Figures 4 and 7e). In contrast, a map analysis reveals a pronounced arcuate

foliation pattern in the Craig Mountain pluton, where foliations are at a low angle to the nearby pluton margin and appear to continuously reorient to an almost perpendicular strike in the pluton center (Figures 4 and 7f).

On some outcrops, relative geometric and temporal relations of mineral fabric to other magmatic structures can be established. For instance, magmatic mineral foliation, in some cases also defined by the alignment of microgranular enclaves, is seen to traverse, with little to no change in orientation, felsic and hornblende-biotite cumulate layers or irregular patches with lobate, diffuse to sharp margins (Figure 8e), and composite mafic-felsic dikes with knife-sharp planar margins (Figure 8d). In other cases, mineral foliation is axial planar to gently folded aplite dikes (Figure 8f).

At map scale, internal pluton foliations are oriented at a high angles to both the Pole Bridge/Hurricane Divide and Hurricane Divide/Craig Mountain interplutonic contacts. On the other hand, magmatic foliations are, in terms of orientation, continuous with host rock markers (lithologic contacts, bedding, and metamorphic foliation; Figure 4) and are thus examples of coupled fabric patterns of *Paterson et al*. [1998]. Local complexities and exceptions to the above do exist, as exemplified by foliations parallel to the local intrusive margin and discordant to host rock structures or by foliations at a high angle to the overall, pluton-wide foliation pattern (Figure 4).

On the microscale, fabrics in the batholith are magmatic to submagmatic in most cases (Parts S1 and S2 in the supporting information) as defined using criteria in *Paterson et al*. [1989] and *Vernon* [2000]. The tonalites (e.g., sample JZ146) typically contain euhedral- to subhedral-zoned andesine phenocrysts up to 7 mm in size, whereas K-feldspar is rare. Amphibole and biotite grains are mostly subhedral with variable size, not exceeding 4.5 mm. Quartz is anhedral and fills the space between other minerals. The quartz grains or aggregates may locally exhibit undulatory extinction and chessboard pattern. The granodiorites (e.g., sample JZ216) show similar microstructure, but contain abundant euhedral to subhedral, patchy zoned tabular grains of K-feldspar and oligoclase, up to 4 mm in size.

The exception is tonalite (sample JZ91) from the eastern margin of the Pole Bridge pluton, which exhibits S-C fabric [e.g., *Berthé et al*., 1979] defined by two oblique shape-preferred orientations of quartz, plagioclase, amphibole, and biotite grains and aggregates. Consistent with this S-C fabric are also asymmetric sigmoidal grains of plagioclase and biotite fish [e.g., *Lister and Snoke*, 1984], all indicating reverse, top-to-the-SW kinematics during submagmatic to high-temperature subsolidus deformation of the tonalite. A similar case is fine-grained amphibole-biotite microtonalite to microdiorite (e.g., sample KV112) possibly representing the chilled margin of the Pole Bridge pluton deformed at submagmatic to high-temperature subsolidus conditions.

6. Anisotropy of Magnetic Susceptibility

6.1. Methodology

The anisotropy of magnetic susceptibility [e.g., *Hrouda*, 1982; *Tarling and Hrouda*, 1993; *Bouchez*, 1997; *Borradaile and Henry*, 1997; *Borradaile and Jackson*, 2004, 2010] was used to describe quantitatively gradients in fabric symmetry, intensity, and orientation in the Wallowa batholith (Figure 9 and Parts S3–S7 in the supporting information). The anisotropy of magnetic susceptibility (AMS) samples were taken at 42 stations: 7 in the Pole Bridge pluton, 15 in the Hurricane Divide pluton, 2 in the Sawtooth stock, and 18 in the Craig Mountain pluton. The samples were taken as oriented blocks and then drilled using a handheld gasoline drill, rotated back to their original (in situ) position, and the orientation of the drilled cores was measured using the standard orientation table. After cutting, the cores yielded 466 standard specimens (cylinder-shaped, 2.1 cm in height and 2.5 cm in diameter; 112 in the Pole Bridge pluton, 20 in the Sawtooth stock, 167 in the Hurricane Divide, and 167 in the Craig Mountain plutons). The AMS was measured using an Agico MFK1-A Multi-function Kappabridge in the Laboratory of Rock Magnetism, Institute of Geology and Paleontology, Charles University in Prague, and statistical treatment and analysis of the AMS data was carried out using the ANISOFT 4.2 program. The calculated AMS parameters are listed in full in Part S4 in the supporting information.

The AMS data are represented by the mean magnetic susceptibility (k_m), degree of anisotropy (P), and shape parameter (T) defined as follows [*Hrouda*, 1982]: $k_m = (k_1 + k_2 + k_3)/3$, $P = k_1/k_3$, and $T = 2ln(k_2/k_3)/ln(k_1/k_3) - 1$,

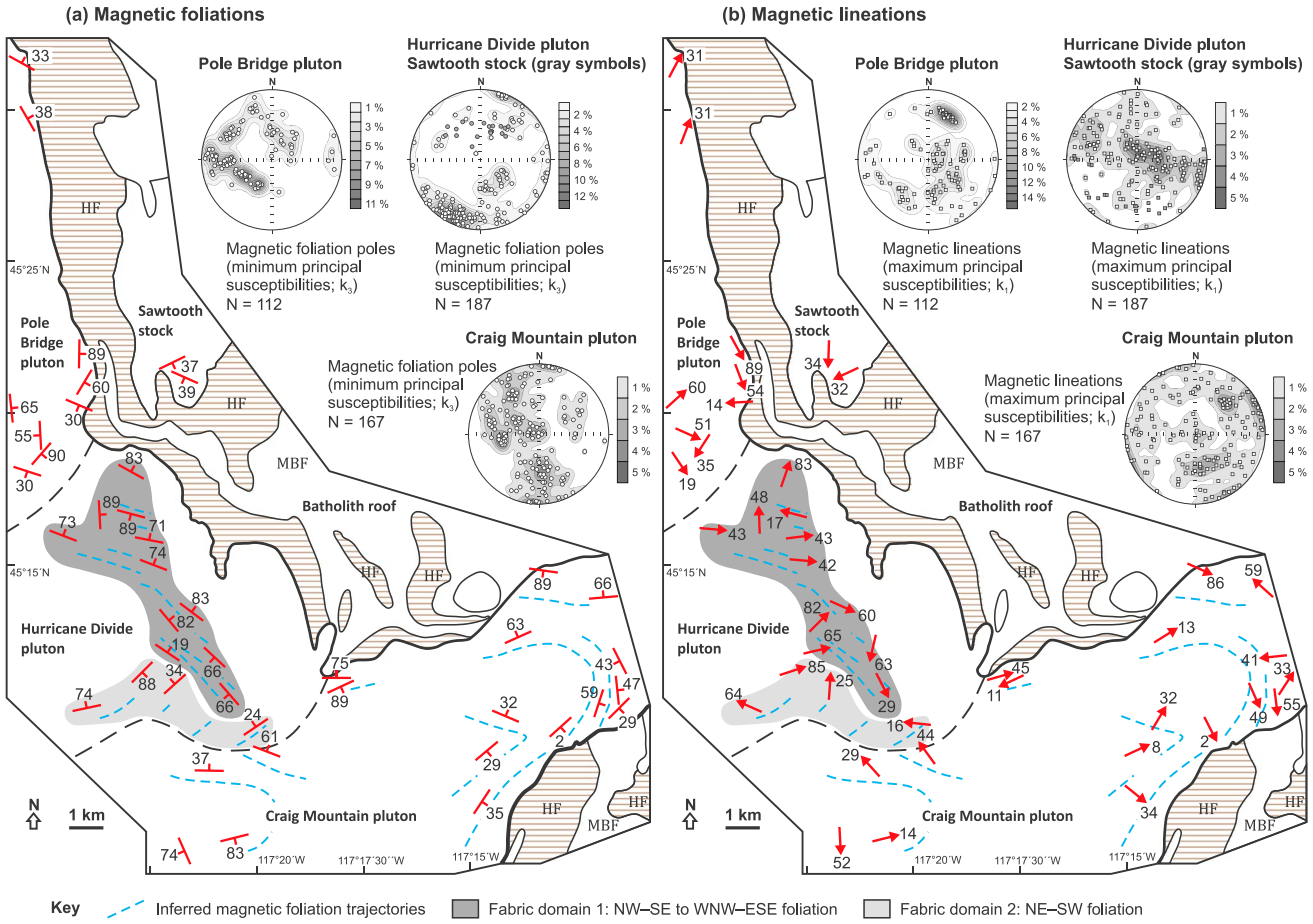

Figure 9. Maps of magnetic foliations and lineations in the component plutons of the northeastern Wallowa batholith. Stereonets (equal area projection, lower hemisphere) show orientations of the maximum and minimum principal susceptibilities. HF–Hurwal Formation and MBF–Martin Bridge Formation.

where $k_1 > k_2 > k_3$ are the principal susceptibilities. The orientations of the magnetic lineations (k_1) and magnetic foliation poles (k_3) are presented in stereonets in the geographic coordinates and as mean values for individual stations on the maps.

6.2. Magnetic Mineralogy

The mean magnetic susceptibility is high, on the orders of 10^{-3} to 10^{-2} in all units (Part S5 in the supporting information), and thus these granitoids (tonalites to granodiorites) can be broadly regarded as ferromagnetic [*Hrouda and Kahan*, 1991; *Bouchez*, 1997] with the main carriers of the AMS being ferromagnetic minerals. However, on five stations (FT96, KV112, JZ106, JZ236, and JZ251), the granitoids have lower susceptibilities on the order of 10^{-4}, suggesting paramagnetic mineralogy.

In order to determine the AMS carriers, variation of susceptibility with temperature was measured on six coarsely powdered specimens in the temperature range from −194°C to 700°C and back to approximately 40°C using the CS-L and CS-4 instruments [*Hrouda*, 1994]. Argon atmosphere was applied to avoid oxidation during heating; the heating rate was approximately 10°C/min. Measurements were performed in the Laboratory of Rock Magnetism, Institute of Geology and Paleontology, Charles University in Prague; the data were statistically treated and plotted using the Cureval software (Agico, Inc.). The resulting thermomagnetic curves are provided in Part S6 in the supporting information.

The analysis corroborates that the main AMS carrier in specimens with high susceptibilities (JZ224/2/2, JZ16/3/4, JZ103/2/1, and KV132/1/1) is magnetite, detected by significant drop in the bulk susceptibility at temperatures from −180°C to −160°C and of 580°C, corresponding to the Verwey transition and Curie

temperature of magnetite, respectively. On the other hand, low-susceptibility specimens (KV112/1/1 and FT96/2/1) exhibit hyperbolic thermomagnetic curves typical of paramagnetic minerals. Both paramagnetic specimens also showed an increase in the bulk susceptibility during cooling, suggesting growth of a secondary ferromagnetic component.

6.3. Magnetic Fabric Parameters and Orientation

The degree of anisotropy of the Pole Bridge pluton specimens ranges widely from 1.025 to 1.929, but the *P* parameter for most of the specimens (82%) is below 1.256 (Part S7 in the supporting information). The susceptibility ellipsoid shapes are almost evenly distributed between oblate (61% of the specimens) and prolate. The exception to the above are two stations, JZ91 and JZ94, where the granitoids have a higher *P* parameter associated with a predominantly prolate AMS ellipsoids (*T* down to -0.161). The other plutons show the *P* parameter mostly not exceeding 1.3, but, unlike the Pole Bridge pluton, most of the specimens in each of these units are oblate (Sawtooth stock, 80%; Hurricane Divide, 87%; and Craig Mountain, 72%) especially those with $P > 1.2$ (Part S7 in the supporting information). The exception is station JZ224 in the Hurricane Divide pluton with high *P* (1.236–1.459) and mostly oblate ellipsoids.

For the high bulk susceptibilities of 10^{-3} to 10^{-2}, the *P* and *T* parameters exhibit systematic spatial variations in the Hurricane Divide and Craig Mountain plutons (Part S7 in the supporting information). In the former, the degree of anisotropy and oblateness of the AMS ellipsoid decrease from the pluton/roof contact inward, defining ~NW-SE trending zones at a high angle to the interpluton contacts. In the latter, zones of comparable *P* and *T* parameters trend ~NE-SW, parallel to the pluton margin; however, the spatial pattern is more irregular. The degree of anisotropy decreases inward from a narrow zone of highly anisotropic granitoids along the southern margin passing into a broad zone of moderately anisotropic granitoids in the pluton center. These variations in the *P* parameter are associated with an increase in the degree of oblateness of the AMS ellipsoids from near-triaxial to weakly oblate. The exception to this trend are two stations with paramagnetic and weakly anisotropic granitoids (Parts S5 and S7 in the supporting information).

The four plutons also differ significantly in the orientation of magnetic fabric. Magnetic foliations in the Pole Bridge pluton strike ~N-S to ~NW-SE and dip moderately to steeply outward, i.e., to the W to NE (Figure 9a). The foliations are thus roughly subparallel to the pluton/host rock contact and to the bedding in siliciclastic metasedimentary rocks of the Hurwal Formation (Figures 4 and 9a). Only along the southern margin of the pluton, magnetic foliations are at a high angle to both the pluton/host rock and Pole Bridge/Hurricane Divide interpluton contact, dipping at an angle of about 30° to the SW (Figure 9a). Magnetic lineations exhibit moderate plunges, and their trends scatter widely to almost all directions but predominantly to the ~NNE (parallel to lineation on bedding planes) and ~SSE (Figure 9b).

In the Hurricane Divide pluton, our analysis revealed two distinct orientations of magnetic fabric. In a northeasterly domain, magnetic foliations are steep and strike ~NW-SE to ~WNW-ESE. They are thus at a high angle to the nearby flat-lying pluton/roof contact but, at the same time, roughly concordant with foliations in the pluton roof (Figures 4 and 9a). Lineations vary from mostly subvertical to shallowly plunging to the ~ESE or ~WNW (Figure 9b). In a southerly domain along the Hurricane Divide/Craig Mountain interpluton contact, magnetic foliations are almost perpendicular to the above, striking ~NE-SW and being associated with variably trending lineations (Figure 9a). Similarly, on the two stations in the Sawtooth stock, magnetic fabric is discordant to the pluton/roof contact: magnetic foliations strike ~WNW-ESE and ~NE-SW and are associated with lineations moderately plunging to the ~SW and ~S, respectively (Figures 9a and 9b).

An entirely different fabric pattern is observed in the Craig Mountain pluton. Along both pluton margins, magnetic foliations are oriented systematically at an angle of about 30°–45° to the nearby pluton/host rock contact, and this angle increases toward pluton center (Figure 9a). In the majority of cases, lineations plunge moderately outward, and their trends are oblique to the contacts (Figure 9b). Altogether, the foliations and lineations define a pronounced asymmetric arcuate pattern in the map with a narrow southeastern and broad northwestern "limbs." This arcuate pattern seems to be continuous with deflected lithologic contacts, bedding, and metamorphic foliation in the host rock on both sides of the pluton (Figure 9a).

7. Discussion

7.1. Structural Interpretation

In terms of orientation of fabric axes, the mesoscopic foliation and lineation defined mostly by paramagnetic mafic minerals (Figure 8a) correspond well to the measured AMS in all three plutons (Figures 4 and 9). The AMS data are interpreted as representing the shape or distribution anisotropy of magnetite grains or aggregates, corroborated by the high bulk susceptibility of most analyzed specimens and by the thermomagnetic measurements (Part S6 in the supporting information). Furthermore, the relative geometric and temporal relations of mineral fabric to other magmatic and host rock structures (Figures 8d–8f) indicate that both the mesoscopic fabrics and AMS in the three plutons record synemplacement to postemplacement increments of regional tectonic strain. Hence, in combination with the existing $^{206}Pb/^{238}U$ ages, our structural and AMS data suggest that the successively emplaced plutons of the Wallowa batholith record three strain regimes, each of unknown duration but certainly active at ~140 Ma, ~131–130 Ma, and ~126 Ma (Figure 10), allowing inferences on the progressive tectonic history of and strain partitioning in the Wallowa terrane during the Early Cretaceous times.

In the northerly ~140 Ma Pole Bridge pluton, mesoscopic and magnetic foliations are subparallel to both the intrusive contact and bedding in the Hurwal Formation, whereas slickenside-type striation on bedding surfaces (inferred to result from simple shear on the bedding planes) and magnetic lineations are oblique to this structural grain (Figures 4, 7, and 9). Together with reverse, top-to-the-SW kinematics observed in the deformed granitoids along pluton margin (Part 2 in the supporting information), this fabric is interpreted as recording early, perhaps preemplacement ~ENE-WSW principal shortening to form the Sawtooth syncline in Domain 1, continued as dip-oblique ~NE-SW shortening and reverse slip during and after final solidification of the northwestern pluton margin (Figure 10a).

In contrast, fabric in the ~130 Ma Hurricane Divide pluton is dominated by ~WNW-ESE foliation and variably, but in most instances steeply, plunging lineation along the mean foliation plane (Figures 4, 7e, and 9b). The inferred synmagmatic strain was oblate, with the fabric intensity and degree of oblateness decreasing from the pluton/host contact inward (Part S7 in the supporting information), and associated with ~NNE-SSW shortening and a vertical stretching component. In the host rock (Domain 2), the latter fabric corresponds to the steepened to overturned bedding and steep metamorphic foliation in the Hurwal and Martin Bridge Formations, respectively, and was associated with refolding of the Sawtooth syncline into ~NW-SE to ~WNW-ESE upright tight to isoclinal folds developed especially in the weak marbles, with fold axial planes subparallel to the magmatic foliation in the pluton (Figures 4 and 10b). In a small domain near the southern margin of the pluton, mesoscopic and magnetic foliations strike ~NE-SW (Figures 4 and 9a), suggesting that the synmagmatic strain was locally more complex. Based on the available information, it is difficult to distinguish whether this latter fabric represents a relic of earlier emplacement-related strain or records two broadly simultaneous but nearly orthogonal shortening directions, ~NW-SE and dominant ~NE-SW, swinging around a common vertical stretching axis [e.g., *Paterson et al*., 2003].

The structural relations indicate that the youngest, 126 Ma Craig Mountain pluton is elongated and axial planar with a regional map-scale bend of host rock markers from the ~NNW-SSE into ~NE-SW trend, tapers southwestward, and bifurcates an originally single unit represented by the coeval Hurricane Divide and Needle Point plutons (Figure 3). Together with the arcuate magmatic and magnetic foliation patterns (Figures 4 and 9a), this suggests that the pluton intruded during increment(s) of crustal scale folding of the adjacent Wallowa terrane about a vertical axis (Figure 10c). Sharp and largely discordant contacts (Figure 4) suggest that emplacement of the pluton was dominated by brittle processes (into a growing crack?) but also by some ductile shortening in marble-dominated lithologies. The latter is evidenced by contact-parallel deflection of host rock markers in concordant portions of the northeastern pluton margin (Figure 4). The internal arcuate fabric pattern is likely composite, resulting from simple shear magma flow into a tensional region along the axial plane of the fold combined with some amount of tectonic shortening across the already emplaced magmatic sheet. The former is consistent with higher-intensity plane-strain fabric along the southeastern margin, whereas the latter produced oblate fabrics along both sides of the pluton (Part S7 in the supporting information). The observed internal fabric pattern is thus more complex than simple theoretical strain variations as predicted for various types of folds [e.g., *Hobbs*, 1971; *Twiss and Moores*, 1992, pp. 314–321, and references therein].

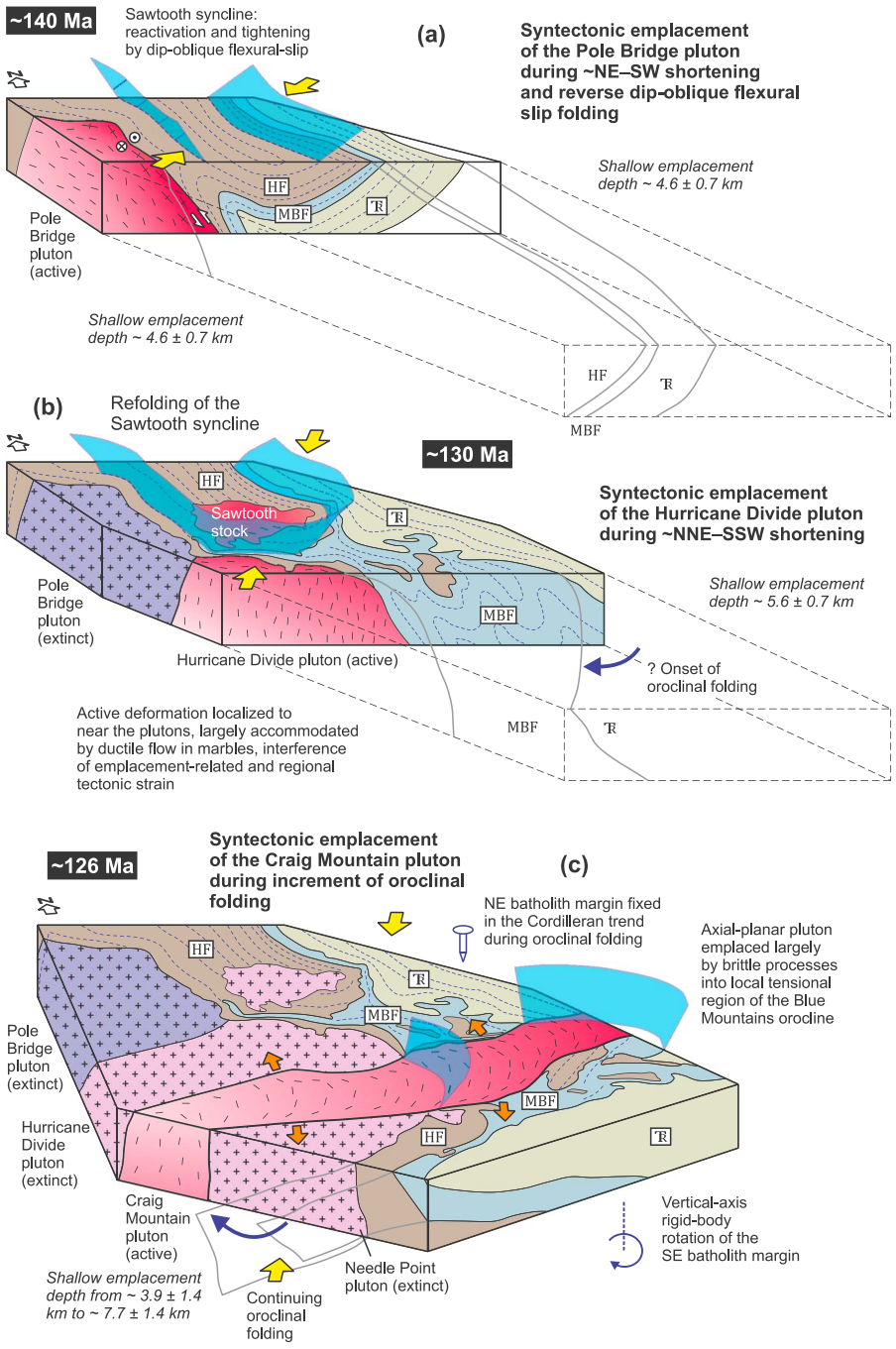

Figure 10. Schematic block diagrams showing the inferred structural and emplacement history of the northeastern Wallowa batholith during the Early Cretaceous times; see text for discussion.

In summary, fabric analysis in the three plutons and their host rocks of the Wallowa terrane suggests that (1) the magmatic and ductile deformation at the exposed shallow crustal level was heterogeneous and largely partitioned into rheologically weak active plutons and their aureoles; (2) deformation was time transgressive, progressing from north to south following the general pattern of magmatic emplacement; and (3) the principal shortening axis rotated counterclockwise from ~NE-SW (in the ~140 Ma Pole Bridge pluton) through ~NNE-SSW (in the ~130 Ma Hurricane Divide pluton) to ~NNW-SSE (in the ~126 Ma Craig Mountain pluton; Figure 10).

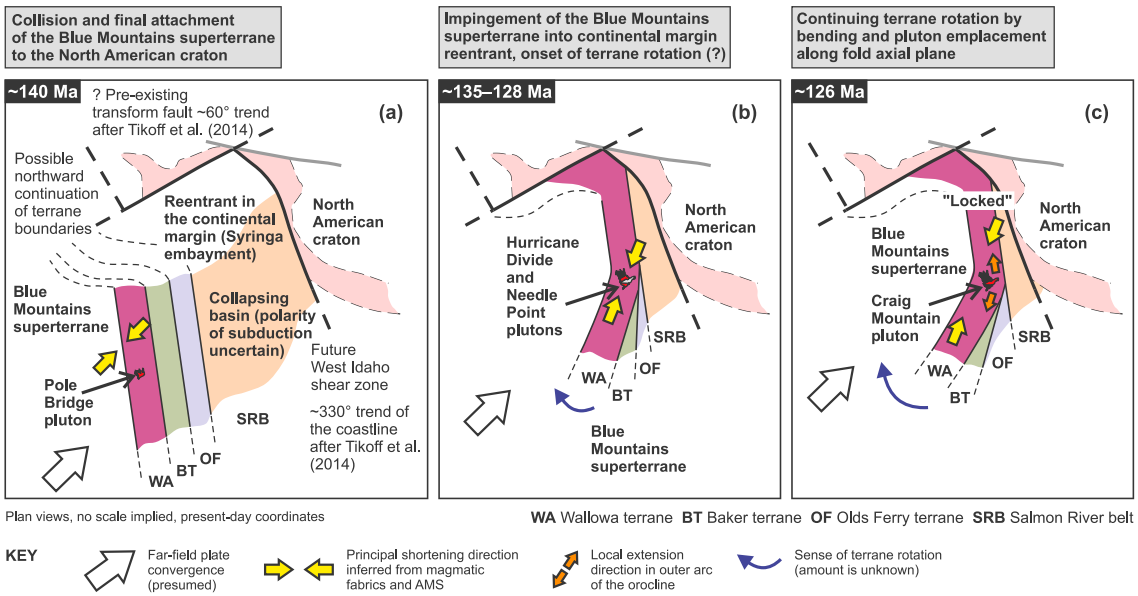

Figure 11. The proposed kinematic model for successive pluton emplacement during terrane collision, impingement into a reentrant in the margin of the North American craton, and incipient oroclinal bending of the Blue Mountains Province during Early Cretaceous right-oblique plate convergence; see text for discussion.

7.2. Inferred Plate Kinematics During Terrane Convergence

Previous structural and geochronologic studies in the Blue Mountains Province suggested (1) amalgamation of the Wallowa and Baker terranes at approximately 162–154 Ma, (2) folding and faulting of the Wallowa-Baker-Olds Ferry terranes and Izee basin by 154 Ma [e.g., *Schwartz et al*., 2010, 2011a, 2011b], (3) thrust loading in the Salmon River belt interpreted as recording collision and final attachment of the Blue Mountains superterrane to cratonic North America at approximately 144–128 Ma [*Selverstone et al*., 1992; *Getty et al*., 1993; *McKay*, 2011], and (4) postcollisional intracontinental shearing along the eastern margin of the accreted terranes spanning from approximately 120 to 80 Ma [e.g., *McClelland et al*., 2000; *Giorgis et al*., 2005, 2008]. Although these studies provided a broad tectonic scenario for the Blue Mountains Province, details of the resulting deformation, changes in regional strain fields through time, and exact timing of these events still remain poorly constrained (see, e.g., *Avé Lallemant* [1995] and *Gray and Oldow* [2005] for discussion).

On the basis of the inferred temporally evolving strain regimes and rotation of the principal strain axes, we propose the following kinematic history of the Wallowa terrane at the time of emplacement of the Wallowa batholith.

The ~NE-SW shortening recorded in the ~140 Ma Pole Bridge pluton and its host rock is broadly coeval with the K-Ar and Sm-Nd garnet ages indicating crustal thickening and thrusting over a time span of about 141–124 Ma in the Salmon River belt [*Selverstone et al*., 1992; *Getty et al*., 1993; *Snee et al*., 1995; *McKay*, 2011; *Stowell et al*., 2014]. We thus interpret this deformation as an early phase of the prolonged attachment of the Blue Mountains "superterrane" to the North American continental margin. The obliquity of the inferred principal shortening direction with respect to the terrane boundaries also implies an overall dextral plate convergence at around 140 Ma (Figures 10a and 11a).

Subsequently, a change in the strain regime and reorientation of the regional strain axes must have occurred between ~140 and ~130 Ma. This can be inferred from fabrics in the ~130 Ma Hurricane Divide pluton which record pure shear with dominant ~NNE-SSW shortening and vertical stretching (thickening) of the crust (Figure 10b). We envisage that the superterrane impinged into a westward concave reentrant in the continental margin as represented by the Syringa embayment (Figures 2 and 11b) [see also *Strayer et al*., 1989]. Our structural data thus indirectly support the notion that the embayment was an inherited, preaccretion feature in the rifted margin of the North American craton [e.g., *Lund et al*., 2008], presumably later reactivated by sinistral transpressional shearing along the approximately 90–70 Ma Orofino shear zone (Figure 2) [*McClelland and Oldow*, 2007].

As a consequence of squeezing the Blue Mountains superterrane into the presumed continental margin reentrant, its northern portion must have become "locked" and difficult to further deform (Figures 10c and 11c). Hence, we assume that the continuing oblique convergence was accommodated by crustal scale folding about a vertical axis, thereby rotating clockwise the southern, still deformable portion of the superterrane (Figures 10c and 11c). The Craig Mountain pluton was emplaced into a local tensional domain along the axial plane, and its internal magmatic fabric records strain during progressive development of this crustal scale fold at around 126 Ma (Figure 10c). Subsequently, ductile deformation became localized mainly along the dextral transpressive Western Idaho shear zone (Figure 2), accommodating continued subduction outboard the Blue Mountains Province until Late Cretaceous times [*McClelland et al*., 2000]. No ductile structures related to these younger events have been identified as yet in the examined portion of the Wallowa terrane, suggesting eastward stepping of deformation through time.

The above inferred strain patterns fit well a general model of granitoid plutonism in developing oroclines [e.g., *Gutiérrez-Alonso et al*., 2011a; *Pastor-Galán et al*., 2012; *Johnston et al*., 2013], whose inner arcs undergo vertical stretching (the Hurricane Divide pluton) and outer arcs undergo horizontal extension (the Craig Mountain pluton). Given that the voluminous plutonism and deformation are closely spatially associated in the Wallowa batholith and that emplacement of the ~140–130 Ma plutons preceded initiation of the orocline, we suggest that thermal weakening from magma emplacement may have played an important role in localizing the hinge of this crustal scale fold. Progressive orocline development commonly triggers delamination of the underlying lithospheric mantle beneath the inner arc [e.g., *Gutiérrez-Alonso et al*., 2004, 2011b; *Weil et al*., 2013]. Mantle delamination beneath the Blue Mountains Province and surrounding areas has been proposed to explain the Miocene flood basalt volcanism of the Columbia River Group [e.g., *Camp and Hanan*, 2008; *Eagar et al*., 2010; *Darold and Humphreys*, 2013, and references therein], and it remains an open question whether this process could have occurred also as early as during the Early/mid-Cretaceous phase of the orocline development.

7.3. Implications for Timing and Mechanism of Rotation of Cordilleran Terranes

The proposed timing and geodynamic causes of the ~E-W bend in terrane boundaries in the Blue Mountain Province have been controversial. The orocline was variously interpreted as (1) being a primary feature and thus recording no rotation [*Taubeneck*, 1966], or resulting from (2) post-middle Eocene oroclinal bending [*Carey*, 1958], (3) Middle Jurassic to Early Cretaceous indentation of the Wrangellia terrane causing lateral escape and rotation of the Stikine (including Wallowa) terrane [*Wernicke and Klepacki*, 1988], (4) Early Cretaceous westward displacement of the Klamath Mountains salient along strike-slip faults [*Ernst*, 2012], (5) Late Cretaceous-Early Tertiary terrane collision [*Tikoff et al*., 2014], or (6) post-Cretaceous Basin-and-Range regional extension [e.g., *Wilson and Cox*, 1980; *Dickinson*, 2002].

Our structural and AMS data and interpretations provide some new temporal and mechanical constraints on this oroclinal rotation. First, we have argued above that the main cause of the fold development, at least during its incipient stages, was oblique oroclinal bending whereby horizontal compressive forces resulting from overall plate convergence acted at an angle to the terrane boundaries (Figures 10 and 11). Second, we propose that the emplacement of the ~130 Ma Hurricane Divide pluton may represent a lower age limit for the oroclinal bending (Figure 11). It remains unresolved whether the vertical stretching as documented in this pluton (Figures 7e and 9b) may represent onset of this process. Nevertheless, we have shown that the progressive folding predated and was active during emplacement of the Craig Mountain pluton (Figure 10c). In summary, these pluton-deformation relationships corroborate that the Blue Mountains orocline probably initiated and at least partly developed earlier than previously thought, during Middle-Early Cretaceous times between approximately 130–126 Ma (Figures 10 and 11).

8. Conclusions

Magmatic to solid state fabrics in the Pole Bridge, Hurricane Divide, and Craig Mountain plutons and coeval deformational structures in their host rocks record three phases of progressive regional deformation in the Wallowa terrane during Early Cretaceous times:

1. The early ~NE-SW terrane-oblique principal shortening is interpreted as recording an early stage of attachment of the welded Blue Mountains superterrane to the North American continental margin during overall right-oblique convergence at around 140 Ma.
2. This deformation switched to pure shear ~NNE-SSW shortening associated with vertical stretching (crustal thickening) and refolding of an earlier kilometer-scale syncline into a series of almost perpendicular smaller-scale tight folds. This event is related to the continued impingement of the superterrane into a westward concave reentrant in the North American continental margin at around 135–128 Ma.
3. Upon impingement, the northern portion of the superterrane became locked and difficult to further deform. The "lock-up" led to reorientation of the principal shortening direction to ~NNW-SSE, and the still deformable southern portion of the superterrane rotated clockwise about vertical axis at around 126 Ma.

The above inferences imply that the main mechanism of the crustal scale fold development was oblique oroclinal bending whereby lateral compressive forces resulting from overall plate convergence acted at an angle to the terrane boundaries and to the continental margin. Pluton fabrics indicate the onset of oroclinal bending at around 130–125 Ma.

Acknowledgments

We greatly appreciate the detailed and constructive comments by Stephen Johnston, Associate Editor, and three anonymous reviewers which helped to improve the original manuscript significantly. Martin Chadima is thanked for the help with processing the thermomagnetic curves. All data related to this manuscript are either directly presented in figures or are available in Parts S1–S7 in the supporting information. Alternatively, the data are available from the authors upon request. This study is part of the Ph.D. research of Filip Tomek, supported by the Grant Agency of the Czech Republic through grant P210/12/1385 (to Jiří Žák), by the Charles University research projects PRVOUK P44 and SVV261203, and by the Czech Academy of Sciences Research Plan RVO67985831. Partial financial support for this work was provided by National Science Foundation grant EAR-0911681 (to Joshua J. Schwartz) and National Science Foundation grant EAR-0911735 (to Kenneth Johnson).

References

Amato, J. M., J. Toro, and T. E. Moore (2004), Origin of the Bering Sea salient, in Orogenic Curvature: Integrating Paleomagnetic and Structural Analyses, in *Geol. Soc. Am. Spec. Pap*, vol. 383, edited by Sussmann, A. J., and A. B. Weil, pp. 131–144, *Geol. Soc. of Am.*, Boulder, Colo., doi:10.1130/0-8137-2383-3(2004)383[131:OOTBSS]2.0.CO;2.

Armstrong, R. L., W. H. Taubeneck, and P. O. Hales (1977), Rb–Sr and K–Ar geochronometry of Mesozoic granitic rocks and their Sr isotopic composition, Oregon, Washington, and Idaho, *Geol. Soc. Am. Bull.*, *88*(3), 397–411, doi:10.1130/0016-7606(1977)88<397:RAKGOM>2.0.CO;2.

Atwater, T. (1970), Implications of plate tectonics for the Cenozoic tectonic evolution of western North America, *Geol. Soc. Am. Bull.*, *81*, 3513–3236, doi:10.1130/0016-7606(1970)81[3513:IOPTFT]2.0.CO;2.

Avé Lallemant, H. G. (1995), Pre-Cretaceous tectonic evolution of the Blue Mountains Province, northeastern Oregon, in *Geology of the Blue Mountains Region of Oregon, Idaho and Washington: Petrology and Tectonic Evolution of pre-Tertiary Rocks of the Blue Mountains Region*, edited by T. L. Vallier and H. C. Brooks, *U.S. Geol. Surv. Prof. Pap.*, *1438*, 271–304, Denver, Colo.

Berthé, D., P. Choukroune, and P. Jegouzo (1979), Orthogneiss, mylonite and non coaxial deformation of granites: The example of the South Armorican shear zone, *J. Struct. Geol.*, *1*, 31–42, doi:10.1016/0191-8141(79)90019-1.

Borradaile, G. J., and B. Henry (1997), Tectonic applications of magnetic susceptibility and its anisotropy, *Earth Sci. Rev.*, *42*(1–2), 49–93, doi:10.1016/S0012-8252(96)00044-X.

Borradaile, G. J., and M. Jackson (2004), Anisotropy of magnetic susceptibility (AMS): Magnetic petrofabrics of deformed rocks, in Magnetic Fabric: Methods and Application, edited by F. Martín-Hernández et al., *Geol. Soc. London Spec. Publ.*, *238*, 299–360, doi:10.1144/GSL.SP.2004.238.01.18.

Borradaile, G. J., and M. Jackson (2010), Structural geology, petrofabrics and magnetic fabrics (AMS, AARM, AIRM), *J. Struct. Geol.*, *32*(10), 1519–1551, doi:10.1016/j.jsg.2009.09.006.

Bouchez, J. L. (1997), Granite is never isotropic: An introduction to AMS studies of granitic rocks, in *Granite: From Segregation of Melt to Emplacement Fabrics*, edited by J. L. Bouchez, D. Hutton, and S. Stephens, pp. 95–112, Kluwer Acad., Amsterdam, doi:10.1007/978-94-017-1717-5_6.

Brooks, H. C., and T. L. Vallier (1978), Mesozoic rocks and tectonic evolution of eastern Oregon and western Idaho, in *Mesozoic Paleogeography of the Western United States*, edited by D. G. Howell and K. A. McDougall, pp. 133–145, The Pacific Section Society of Economic Paleontologists and Mineralogists, Los Angeles, Calif.

Camp, V. E., and B. B. Hanan (2008), A plume-triggered delamination origin for the Columbia River Basalt Group, *Geosphere*, *4*(3), 480–495, doi:10.1130/GES00175.1.

Carey, S. W. (1958), The tectonic approach to continental drift, in *Continental Drift: A Symposium*, edited by S. W. Carey, pp. 177–363, Univ. of Tasmania, Hobart.

Coney, P. J., J. L. Jones, and J. W. H. Monger (1980), Cordilleran suspect terranes, *Nature*, *288*, 329–333, doi:10.1038/288329a0.

Darold, A., and E. Humphreys (2013), Upper mantle seismic structure beneath the Pacific Northwest: A plume-triggered delamination origin for the Columbia River flood basalt eruptions, *Earth Planet. Sci. Lett.*, *365*, 232–242, doi:10.1016/j.epsl.2013.01.024.

Dickinson, W. R. (1979), Mesozoic forearc basin in central Oregon, *Geology*, *7*, 166–170, doi:10.1130/0091-7613(1979)7<166:MFBICO>2.0.CO;2.

Dickinson, W. R. (2002), The Basin and Range Province as a composite extensional domain, *Int. Geol. Rev.*, *44*(1), 1–38, doi:10.2747/0020-6814.44.1.1.

Dickinson, W. R. (2004), Evolution of the North American Cordillera, *Annu. Rev. Earth Planet. Sci.*, *32*, 13–45, doi:10.1146/annurev.earth.32.101802.120257.

Dorsey, R. J., and T. A. LaMaskin (2007), Stratigraphic record of Triassic–Jurassic collisional tectonics in the Blue Mountains Province, northeastern Oregon, *Am. J. Sci.*, *307*, 1167–1193, doi:10.2475/10.2007.03.

Dorsey, R. J., and T. A. LaMaskin (2008), Mesozoic collision and accretion of oceanic terranes in the Blue Mountains Province of northeastern Oregon: New insights from the stratigraphic record, in *Circum-Pacific Tectonics, Geologic Evolution, and Ore Deposits, Arizona Geol. Soc. Digest*, vol. 22, edited by J. E. Spencer and S. R. Titley, pp. 325–332, Arizona Geological Society, Tucson.

Eagar, K. C., M. J. Fouch, and D. E. James (2010), Receiver function imaging of upper mantle complexity beneath the Pacific Northwest, United States, *Earth Planet. Sci. Lett.*, *297*, 141–153, doi:10.1016/j.epsl.2010.06.015.

Engebretson, D. C., A. Cox, and R. G. Gordon (1985), Relative motions between oceanic and continental plates in the Pacific basin, *Geol. Soc. Am. Spec. Pap.*, *206*, 1–59, doi:10.1130/SPE206-p1.

Ernst, W. G. (2012), Earliest Cretaceous Pacificward offset of the Klamath Mountains salient, NW California–SW Oregon, *Lithosphere*, *5*(1), 151–159, doi:10.1130/L247.1.

Ferns, M. L., and H. C. Brooks (1995), The Bourne and Greenhorn subterranes of the Baker Terrane, northeastern Oregon; Implications for the evolution of the Blue Mountains island arc system, in *Geology of the Blue Mountains Region of Oregon, Idaho and Washington: Petrology and Tectonic Evolution of pre-Tertiary Rocks of the Blue Mountains Region*, edited by T. L. Vallier and H. C. Brooks, *U.S. Geol. Surv. Prof. Pap.*, *1438*, 331–358, Denver, Colo.

Getty, S. R., J. Selverstone, B. P. Wernicke, S. B. Jacobsen, and E. Aliberti (1993), Sm–Nd dating of multiple garnet growth events in an arc–continent collision zone, northwestern U.S. Cordillera, *Contrib. Mineral. Petrol.*, *115*, 45–47, doi:10.1007/BF00712977.

Giorgis, S., B. Tikoff, and W. McClelland (2005), Missing Idaho arc: Transpressional modification of the $^{87}Sr/^{86}Sr$ transition on the western edge of the Idaho batholith, *Geology*, *33*, 469–472, doi:10.1130/G20911.1.

Giorgis, S., W. C. McClelland, A. Fayon, B. S. Singer, and B. Tikoff (2008), Timing of deformation and exhumation in the western Idaho shear zone, McCall, Idaho, *Geol. Soc. Am. Bull.*, *120*(9–10), 1119–1133, doi:10.1130/B26291.1.

Glen, J. M. G. (2004), A kinematic model for the southern Alaska orocline based on regional fault patterns, in *Orogenic Curvature: Integrating Paleomagnetic and Structural Analyses*, edited by A. J. Sussmann and A. B. Weil, *Geol. Soc. Am. Spec. Pap.*, *383*, 161–172, Boulder, Colo., doi:10.1130/0-8137-2383-3(2004)383[161:AKMFTS]2.0.CO;2.

Gray, K. D., and J. S. Oldow (2005), Contrasting structural histories of the Salmon River belt and Wallowa terrane: Implications for terrane accretion in northeastern Oregon and west-central Idaho, *Geol. Soc. Am. Bull.*, *117*(5–6), 687–706, doi:10.1130/B25411.1.

Greenwood, W. R., and R. R. Reid (1969), The Columbia Arc: New evidence for pre-Tertiary rotation, *Geol. Soc. Am. Bull.*, *80*, 1797–1800, doi:10.1130/0016-7606(1969)80[1797:TCANEF]2.0.CO;2.

Grommé, C. S., M. E. Beck, and D. C. Engebretson (1986), Paleomagnetism of the Tertiary Clarno Formation of central Oregon and its significance for the tectonic history of the Pacific Northwest, *J. Geophys. Res.*, *91*(B14), 14,089–14,103, doi:10.1029/JB091iB14p14089.

Gutiérrez-Alonso, G., J. Fernández-Suárez, A. B. Weil (2004), Orocline triggered lithospheric delamination, in *Orogenic Curvature: Integrating Paleomagnetic and Structural Analyses*, edited by A. J. Sussmann and A. B. Weil, *Geol. Soc. Am. Spec. Pap.*, *383*, 121–130, Boulder, Colo., doi:10.1130/0-8137-2383-3(2004)383[121:OTLD]2.0.CO;2.

Gutiérrez-Alonso, G., J. Fernández-Suárez, T. E. Jeffries, S. T. Johnston, D. Pastor-Galán, J. B. Murphy, M. P. Franco, and J. C. Gonzalo (2011a), Diachronous post-orogenic magmatism within a developing orocline in Iberia, European Variscides, *Tectonics*, *30*, TC5008, doi:10.1029/2010TC002845.

Gutiérrez-Alonso, G., J. B. Murphy, J. Fernández-Suárez, A. B. Weil, M. Piedad Franco, and J. C. Gonzalo (2011b), Lithospheric delamination in the core of Pangea: Sm–Nd insights from the Iberian mantle, *Geology*, *39*(2), 155–158, doi:10.1130/G31468.1.

Hamilton, W. (1969), Mesozoic California and the underflow of Pacific mantle, *Geol. Soc. Am. Bull.*, *80*, 2409–2430, doi:10.1130/0016-7606(1959)70[1119:COGFWL]2.0.CO;2.

Hamilton, W., and W. B. Myers (1966), Cenozoic tectonics of the western United States, *Rev. Geophys.*, *4*(4), 509–549, doi:10.1029/RG004i004p00509.

Hildebrand, R. S. (2009), Did westward subduction cause Cretaceous–Tertiary orogeny in the North American Cordillera?, *Geol. Soc. Am. Spec. Pap.*, *457*, 1–71, doi:10.1130/2009.2457.

Hildebrand, R. S. (2013), Mesozoic assembly of the North American Cordillera, *Geol. Soc. Am. Spec. Pap.*, *495*, 1–169, doi:10.1130/9780813724959.

Hillhouse, J. W., C. S. Grommé, and T. L. Vallier (1982), Paleomagnetism and Mesozoic tectonics of the Seven Devils volcanic arc in northeastern Oregon, *J. Geophys. Res.*, *87*(B5), 3777–3794, doi:10.1029/JB087iB05p03777.

Hobbs, B. E. (1971), The analysis of strain in folded layers, *Tectonophysics*, *11*(5), 329–375, doi:10.1016/0040-1951(71)90025-4.

Housen, B. A., and R. J. Dorsey (2005), Paleomagnetism and tectonic significance of Albian and Cenomanian turbidites, Ochoco Basin, Mitchell Inlier, central Oregon, *J. Geophys. Res.*, *110*, B07102, doi:10.1029/2004JB003458.

Hrouda, F. (1982), Magnetic anisotropy of rocks and its application in geology and geophysics, *Geophys. Surv.*, *5*(1), 37–82, doi:10.1007/BF01450244.

Hrouda, F. (1994), A technique for the measurement of thermal changes of magnetic susceptibility of weakly magnetic rocks by the CS-2 apparatus and KLY-2 Kappabridge, *Geophys. J. Int.*, *118*(3), 604–612, doi:10.1111/j.1365-246X.1994.tb03987.x.

Hrouda, F., and Š. Kahan (1991), The magnetic fabric relationship between sedimentary and basement nappes in the High Tatra Mountains, N. Slovakia, *J. Struct. Geol.*, *13*(4), 431–442, doi:10.1016/0191-8141(91)90016-C.

Johnson, K., C. G. Barnes, and C. A. Miller (1997), Petrology, geochemistry, and genesis of high-Al tonalite and trondhjemites of the Cornucopia stock, Blue Mountains, northeastern Oregon, *J. Petrol.*, *38*, 1585–1611, doi:10.1093/petroj/38.11.1585.

Johnson, K., C. G. Barnes, J. M. Browning, and H. R. Karlsson (2002), Petrology of iron-rich magmatic segregations associated with strongly peraluminous trondhjemite in the Cornucopia stock, northeastern Oregon, *Contrib. Mineral. Petrol.*, *142*, 564–581, doi:10.1007/s00410-001-0311-z.

Johnson, K., J. J. Schwartz, J. L. Wooden, L. J. O'Driscoll, and R. C. Jeffcoat (2011), The Wallowa batholith: New Pb/U (SHRIMP–RG) ages place constraints on arc magmatism and crustal thickening in the Blue Mountains Province, NE Oregon [Abstracts with Programs], *Geol. Soc. Am.*, *43*(4), 5.

Johnston, S. T. (2001), The Great Alaskan Terrane Wreck: Reconciliation of paleomagnetic and geological data in the northern Cordillera, *Earth Planet. Sci. Lett.*, *193*, 259–272, doi:10.1016/S0012-821X(01)00516-7.

Johnston, S. T. (2008), The Cordilleran ribbon continent of North America, *Annu. Rev. Earth Planet. Sci.*, *36*, 495–530, doi:10.1146/annurev.earth.36.031207.124331.

Johnston, S. T., and S. Acton (2003), The Eocene Southern Vancouver Island orocline—A response to seamount accretion and the cause of fold-and-thrust belt and extensional basin formation, *Tectonophysics*, *365*(1–4), 165–183, doi:10.1016/S0040-1951(03)00021-0.

Johnston, S. T., A. B. Weil, and G. Gutiérrez-Alonso (2013), Oroclines: Thick and thin, *Geol. Soc. Am. Bull.*, *125*(5–6), 643–663, doi:10.1130/B30765.

Krauskopf, K. B. (1943), The Wallowa batholith, *Am. J. Sci.*, *241*(10), 607–628, doi:10.2475/ajs.241.10.607.

LaMaskin, T. A., R. J. Dorsey, and J. D. Vervoort (2008), Tectonic controls on mudrock geochemistry, mesozoic rocks of eastern Oregon and western Idaho, U.S.A.: Implications for Cordilleran tectonics, *J. Sediment. Res.*, *78*(12), 765–783, doi:10.2110/jsr.2008.087.

LaMaskin, T. A., J. J. Schwartz, R. J. Dorsey, A. W. Snoke, K. Johnson, and J. D. Vervoort (2009), Mesozoic sedimentation, magmatism, and tectonics in the Blue Mountains Province, northeastern Oregon, *Geol. Soc. Am. Field Guide*, *15*, 1–17, doi:10.1130/2009.fld015(09).

LaMaskin, T. A., J. D. Vervoort, R. J. Dorsey, and J. E. Wright (2011), Early Mesozoic paleogeography and tectonic evolution of the western United States: Insights from detrital zircon U–Pb geochronology, Blue Mountains Province, northeastern Oregon, *Geol. Soc. Am. Bull.*, *123*(9–10), 1939–1965, doi:10.1130/B30260.1.

Lister, G. S., and A. W. Snoke (1984), S–C mylonites, *J. Struct. Geol.*, *6*, 617–638, doi:10.1016/0191-8141(84)90001-4.

Lund, K., J. N. Aleinikoff, E. Y. Yacob, D. M. Unruh, and C. M. Fanning (2008), Coolwater culmination: Sensitive high-resolution ion microprobe (SHRIMP) U-Pb and isotopic evidence for continental delamination in the Syringa Embayment, Salmon River suture, Idaho, *Tectonics*, *27*, TC2009, doi:10.1029/2006TC002071.

Manduca, C. A., L. T. Silver, and H. P. Taylor (1992), $^{87}Sr/^{86}Sr$ and $^{18}O/^{16}O$ isotopic systematics and geochemistry of granitoids plutons across a steeply-dipping boundary between contrasting lithospheric blocks in western Idaho, *Contrib. Mineral. Petrol.*, *109*, 355–372, doi:10.1007/BF00283324.

Manduca, C. A., M. A. Kuntz, and L. T. Silver (1993), Emplacement and deformation history of the western margin of the Idaho batholith near McCall, Idaho: Influence of a major terrane boundary, *Geol. Soc. Am. Bull.*, *105*(6), 749–765, doi:10.1130/0016-7606(1993)105<0749:EADHOT>2.3.CO;2.

McClelland, W. C., and J. S. Oldow (2007), Late Cretaceous truncation of the western Idaho shear zone in the central North American Cordillera, *Geology*, *35*(8), 723–726, doi:10.1130/G23623A.1.

McClelland, W. C., B. Tikoff, and C. A. Manduca (2000), Two-phase evolution of accretionary margins: Examples from the North American Cordillera, *Tectonophysics*, *326*, 37–55, doi:10.1016/S0040-1951(00)00145-1.

McKay, M. P. (2011), Pressure–temperature–time paths, prograde garnet growth, and protolith of tectonites from a polydeformational, polymetamorphic terrane: Salmon River suture zone, west-central Idaho, MS thesis, Univ. of Alabama.

McWilliams, M., and Y. P. Li (1985), Oroclinal bending of the southern Sierra Nevada batholith, *Science*, *230*, 172–175, doi:10.1126/science.230.4722.172.

Monger, J. W. H. (1997), Plate tectonics and northern Cordilleran geology: An unfinished revolution, *Geosci. Canada*, *24*, 189–198, doi:10.12789/gs.v24i4.3953.

Mortimer, N. (1986), Late Triassic, arc-related, potassic igneous rocks in the North American Cordillera, *Geology*, *14*(12), 1035–1038, doi:10.1130/0091-7613(1986)14<1035:LTAPIR>2.0.CO;2.

Nolf, B. (1966), Structure and stratigraphy of part of the northern Wallowa Mountains, northeast Oregon, PhD dissertation, Princeton Univ., N. J.

Pastor-Galán, D., G. Gutiérrez-Alonso, G. Zulauf, and F. Zanella (2012), Analogue modeling of lithospheric-scale orocline buckling: Constraints on the evolution of the Iberian–Armorican Arc, *Geol. Soc. Am. Bull.*, *124*(7–8), 1293–1309, doi:10.1130/B30640.1.

Paterson, S. R., R. H. Vernon, and O. T. Tobisch (1989), A review of criteria for identification of magmatic and tectonic foliations in granitoids, *J. Struct. Geol.*, *11*(3), 349–363, doi:10.1016/0191-8141(89)90074-6.

Paterson, S. R., T. K. Fowler, K. L. Schmidt, A. S. Yoshinobu, E. S. Yuan, and R. B. Miller (1998), Interpreting magmatic fabric patterns in plutons, *Lithos*, *44*(1–2), 53–82, doi:10.1016/S0024-4937(98)00022-X.

Paterson, S. R., J. Onézime, L. Teruya, and J. Žák (2003), Quadruple-pronged enclaves: Their significance for the interpretation of multiple magmatic fabrics in plutons, *J. Virt. Explor.*, *10*, 15–30.

Patton, W. W., and I. L. Tailleur (1977), Evidence in the Bering Strait region for differential movement between North America and Eurasia, *Geol. Soc. Am. Bull.*, *88*, 1298–1304, doi:10.1130/0016-7606(1977)88<1298:EITBSR>2.0.CO;2.

Piercey, S. J., and M. Colpron (2009), Composition and provenance of the Snowcap assemblage, basement to the Yukon–Tanana terrane, northern Cordillera: Implications for Cordilleran crustal growth, *Geosphere*, *5*(5), 439–464, doi:10.1130/GES00505.1.

Sarewitz, D. (1983), Seven Devils terrane: Is it really a piece of Wrangellia?, *Geology*, *11*(11), 634–637, doi:10.1130/0091-7613(1983)11<634:SDTIIR>2.0.CO;2.

Schmidt, K. L., R. F. Burmeister, P. K. Link, and C. M. Fanning (2003), New constraints on the western Idaho orocline: A primary feature in the Mesozoic collision zone or result of strike-slip modification? [Abstracts with Programs], *Geol. Soc. Am.*, *35*(6), 559.

Schmidt, K. L., R. S. Lewis, R. M. Gaschnig, and J. Vervoort (2009), Testing hypotheses on the origin of the Syringa embayment in the Salmon River suture zone, western Idaho, USA [Abstracts with Programs], *Geol. Soc. Am.*, *41*, 223.

Schwartz, J. J., and K. Johnson (2014), Construction of Phanerozoic continental crust in the Blue Mountains Province by tectonic assembly and magmatic addition [Abstracts with Programs], *Geol. Soc. Am.*, *43*(5), 647.

Schwartz, J. J., A. W. Snoke, C. D. Frost, C. G. Barnes, L. P. Gromet, and K. Johnson (2010), Analysis of the Wallowa–Baker terrane boundary: Implications for tectonic accretion in the Blue Mountains Province, northeastern Oregon, *Geol. Soc. Am. Bull.*, *122*(3–4), 517–536, doi:10.1130/B26493.1.

Schwartz, J. J., A. W. Snoke, F. Cordey, K. Johnson, C. D. Frost, C. G. Barnes, T. A. LaMaskin, and J. L. Wooden (2011a), Late Jurassic magmatism, metamorphism, and deformation in the Blue Mountains Province, northeast Oregon, *Geol. Soc. Am. Bull.*, *123*(9–10), 2083–2111, doi:10.1130/B30327.1.

Schwartz, J. J., K. Johnson, E. A. Miranda, and J. L. Wooden (2011b), The generation of high Sr/Y plutons following Late Jurassic arc–arc collision, Blue Mountains Province, NE Oregon, *Lithos*, *126*, 22–41, doi:10.1016/j.lithos.2011.05.005.

Schwartz, J. J., K. Johnson, P. Mueller, J. Valley, A. Strickland, and J. L. Wooden (2014), Time scales and processes of Cordilleran batholith construction and high-Sr/Y magmatic pulses: Evidence from the Bald Mountain batholith, northeastern Oregon, *Geosphere*, *10*, 1456–1481, doi:10.1130/GES01033.1.

Selverstone, J., B. P. Wernicke, and E. A. Aliberti (1992), Intracontinental subduction and hinged unroofing along the Salmon River suture zone, west central Idaho, *Tectonics*, *11*(1), 124–144, doi:10.1029/91TC02418.

Sigloch, K., and M. G. Mihalynuk (2013), Intra-oceanic subduction shaped the assembly of Cordilleran North America, *Nature*, *496*, 50–56, doi:10.1038/nature12019.

Snee, L. W., K. Lund, J. F. Sutter, D. E. Balcer, and K. V. Evans (1995), An $^{40}Ar/^{39}Ar$ chronicle of the tectonic development of the Salmon River suture zone, western Idaho, in *Geology of the Blue Mountains Region of Oregon, Idaho and Washington: Petrology and Tectonic Evolution of pre-Tertiary Rocks of the Blue Mountains Region*, edited by T. L. Vallier and H. C. Brooks, *U.S. Geol. Surv. Prof. Pap.*, *1438*, 359–414, Denver, Colo.

Stanley, G. D., C. A. McRoberts, and M. T. Whalen (2008), Stratigraphy of the Triassic Martin Bridge Formation, Wallowa terrane: Stratigraphy and depositional setting, in *The Terrane Puzzle: New Perspectives on Paleontology and Stratigraphy From the North American Cordillera*, edited by R. B. Blodgett and G. D. Stanley, *Geol. Soc. Am. Spec. Pap.*, *442*, 227–250, Boulder, Colo., doi:10.1130/2008.442(12).

Stowell, H., M. P. McKay, J. J. Schwartz, and D. R. Gray (2014), Loading and metamorphism within the Salmon River suture zone, west-central Idaho [Abstracts with Programs], *Geol. Soc. Am.*, *43*(5), 647.

Strayer, L. M., D. W. Hyndman, J. W. Sears, and P. E. Myers (1989), Direction and shear sense during suturing of the Seven Devils–Wallowa terrane against North America in western Idaho, *Geology*, *17*(11), 1025–1028, doi:10.1130/0091-7613(1989)017<1025:DASSDS>2.3.CO;2.

Tarling, D. H., and F. Hrouda (1993), *The Magnetic Anisotropy of Rocks*, Chapman and Hall, London.

Taubeneck, W. H. (1964), Cornucopia stock, Wallowa Mountains, northeastern Oregon: Field relationships, *Geol. Soc. Am. Bull.*, *75*(11), 1093–1116, doi:10.1130/0016-7606(1964)75[1093:CSWMNO]2.0.CO;2.

Taubeneck, W. H. (1966), An evaluation of tectonic rotation in the Pacific Northwest, *J. Geophys. Res.*, *71*(8), 2113–2120, doi:10.1029/JZ071i008p02113.

Taubeneck, W. H. (1987), The Wallowa Mountains, northeast Oregon, in *Geol. Soc. Am. Centennial Field Guide: Cordilleran Section*, edited by M. L. Hill, pp. 327–332, *Geol. Soc. of Am.*, Boulder, Colo., doi:10.1130/0-8137-5401-1.327.

Tikoff, B., P. Kelso, T. Stetson-Lee, A. Byerly, R. M. Gaschnig, J. D. Vervoort, and A. P. Rinna (2014), The role of the Precambrian rifted margin on Cretaceous-aged deformation[Abstracts with Programs], *Geol. Soc. Am.*, *46*(5), 18.

Twiss, R. J., and E. M. Moores (1992), *Structural Geology*, 532 pp., W.H. Freeman and Company, New York.

Vallier, T. L. (1995), Petrology of pre-Tertiary igneous rocks in the Blue Mountains region of Oregon, Idaho, and Washington: Implications for the geologic evolution of a complex island arc, in *Geology of the Blue Mountains Region of Oregon, Idaho and Washington: Petrology and Tectonic Evolution of pre-Tertiary Rocks of the Blue Mountains Region*, edited by T. L. Vallier and H. C. Brooks, *U.S. Geol. Surv. Prof. Pap.*, *1438*, 125–219, Denver, Colo.

Vernon, R. H. (2000), Review of microstructural evidence of magmatic and solid-state flow, *Electron. Geosci.*, *5*(2), 1–23, doi:10.1007/s10069-000-0002-3.

Walker, G. W. (1979), Reconnaissance geologic map of the Oregon part of the Grangeville quadrangle, Baker, Union, Umatilla, and Wallowa Counties, Oregon, scale 1:250,000 U.S. Geol. Surv. miscellaneous investigations series map No. I-1116.

Weil, A. B., G. Gutiérrez-Alonso, S. T. Johnston, and D. Pastor-Galán (2013), Kinematic constraints on buckling a lithospheric-scale orocline along the northern margin of Gondwana: A geologic synthesis, *Tectonophysics*, *582*, 25–49, doi:10.1016/j.tecto.2012.10.006.

Weis, P. L., J. L. Gualtieri, W. F. Cannon, E. T. Tuchek, A. B. McMahan, and F. E. Federspiel (1976), Mineral resources of the Eagle Cap Wilderness and adjacent areas, Oregon U. S. Geol. Surv. Bull., 1385–E, 1–100.

Wernicke, B., and D. W. Klepacki (1988), Escape hypothesis for the Stikine block, *Geology*, *16*(5), 461–464, doi:10.1130/0091-7613(1988)016<0461:EHFTSB>2.3.CO;2.

Wilson, D., and A. Cox (1980), Paleomagnetic evidence for tectonic rotation of Jurassic plutons in Blue Mountains, eastern Oregon, *J. Geophys. Res.*, *85*(NB7), 3681–3689, doi:10.1029/JB085iB07p03681.

Žák, J., K. Verner, K. Johnson, and J. J. Schwartz (2012a), Magnetic fabric of Late Jurassic arc plutons and kinematics of terrane accretion in the Blue Mountains, northeastern Oregon, *Gondwana Res.*, *22*(1), 341–352, doi:10.1016/j.gr.2011.09.013.

Žák, J., K. Verner, K. Johnson, and J. J. Schwartz (2012b), Magma emplacement process zone preserved in the roof of a large Cordilleran batholith, Wallowa Mountains, northeastern Oregon, *J. Volcanol. Geotherm. Res.*, *227–228*, 61–75, doi:10.1016/j.jvolgeores.2012.03.001.